The Air Cavity, f-holes and Helmholtz Resonance of a Violin or Viola

John Coffey, Cheshire, UK.

2013

1 Introduction

If the man-in-the-street were asked 'Why are there two slots in the top of a violin?' he might answer 'To let the sound out'. Is he correct? If so, is this all there is to it? Although the shape, size and position of the two f-holes have been established through centuries of practice, we can still ask how important they are to the quality of sound produced, and whether other holes in other places would work just as well.

This is the fifth article in a series describing my personal investigations into the acoustics of the violin and viola. Previous articles have used experiment and finite element analysis with the LISA and Strand7 programs to investigate the normal modes of vibration of the wooden components of these stringed instruments, starting with single free flat plates. In these studies the wood was considered to be in vacuum as far as its vibrations are concerned. This present article considers the air inside the belly of the instrument, its vibration in and out of the two f-holes, and its interaction with the enclosing wooden box.

Pioneering studies of the physics of the violin by Carleen Hutchins, Frederick Saunders and several others, reviewed briefly in §4, have described a series of air resonances in a violin, viola or 'cello termed A0, A1, A2, etc. On a violin A0, the lowest, is at about 270 Hz and A1 at about 470 Hz. All except A0 correspond to standing waves inside the cavity, similar to those in an organ pipe. By contrast, at A0 the instrument acts much like a classic Helmholtz resonator in which a plug of air vibrates in and out of each f-hole, with the air inside acting as a spring, expanding and contracting in volume. A Helmholtz resonance is also produced by blowing across the neck of a wine bottle. The pitch of the note depends on the volume of the air reservoir and (unlike an organ pipe) not on its length *per se*. Of course, the air in a violin is only set in motion through the vibration of the wooden box structure, so there must be coupling between the air and the thin wooden walls. A0 is described as crucial for strengthening the loudness of notes on the lowest two strings (G and D on violin, C and G on viola) since the lowest wood resonance is typically a musical fifth higher.

To orient us and show the scope of the topic, I start in §2 with some experimental measurements on a simplified model of a violin – a wooden box with only one flexible plate and only one hole into the cavity, driven electro-mechanically by a sinusoidal force from a signal generator. Listening with an external microphone, we obtain amplitude-frequency curves which map the sound radiated as the frequency is swept. These curves have a rich structure and together they pose a challenge to analytical theory and numerical modelling, to explain their many peaks and troughs. Some may will

be due primarily to the normal modes of the wooden plates, some to the air cavity, and some may depend in frequency and amplitude on coupling between wood and air.

From these amplitude-frequency spectra we pick out the Helmholtz resonance, which is the central topic of this article. I hope to quantify the wider complexities in future articles. In §3 I describe my own experiments to observe and measure the Helmholtz and other air resonances in violins and violas. There is a large literature on acoustic resonators dating back to Helmholtz's original papers of the 1880s and Lord Rayleigh's theoretical analysis in volume II of his monumental 'Theory of Sound'. The literature broadly falls into two categories:

1. studies of the importance of A0 and other resonances on the musical tone and loudness of violins,

2. studies of how the frequency of any Helmholtz resonator, not necessarily a violin, is determined by the volume and shape of the cavity and the area, height and shape of the neck opening.

The brief review in §4 deals with category 1, mainly the work of Carleen Hutchins and Frederick Saunders on the tone of violins. Category 2 studies are considered in the later sections of this paper, from §5 onwards. In §5 I derive the classic Helmholtz frequency formula for the case where the cavity has rigid walls. Most traditional calculations assume a simple shape of opening and neck of the Helmholtz resonator. I have examined a range of shapes with the LISA finite element program which can solve the relevant Helmholtz acoustic wave equation assuming rigid walls. These start in §6 with the acoustically simple case of a wine bottle. §7 describes a sequence of experimental and corresponding FEA studies of a rectangular plywood box with a volume about that of a violin into which apertures of various sizes and shapes are cut. Finally §8 discusses the coupling between the air cavity and flexible elastic walls, presenting experimental results to show that flexible walls can lower A0 to at least 65% of its value when the walls are rigid.

2 'Letting the sound out'

I start by describing the last set of experiments I carried out for this article because it sets the scene for all the subsequent discussion. Acoustic measurements were made on a wooden box which I will call Box C; it will be referred to in later sections, where further details are given. It is the cuboidal box in Figure 1 with roughly the dimensions of a violin, being internally 340 mm by 160 mm by 45 mm. It was initially made of $2 \cdot 91$ mm thick 3-plywood but then clad on all sides except the back with thick MDF[1] board to make those faces almost rigid. A window had been cut in the MDF of the top plate to leave a small area of the 3-ply exposed, and into this had been cut a slot about 53 mm long and 14 mm wide, through into the cavity. Thus the MDF is clear of the aperture by about 15 mm all round, and the thickness of the plate at and immediately around the aperture is only $2 \cdot 91$ mm. At a later stage I lengthened and widened this single slot to about 61 mm by 28 mm (Figure 1). The box is a highly simplified model of a violin.

2.1 The observed amplitude-frequency response

The box was driven into oscillation and the radiated sound recorded using the arrangement in Figure 2. The electromagnetic exciter, which had been used in previous experiments described in www.mathstudio.co.uk, was positioned in the centre of the flexible back plate and held lightly with adhesive tape to stop it meandering sideways. The box was placed flat on soft furnishings, exciter underneath, aperture on top and, for the first set of measurements, was padded around with cushions

---

[1]Medium density fibreboard, 13 or 19 mm thick

Figure 1: The wooden box, clad in MDF, with a cut-out around the aperture (61 by 28 mm) in the top plywood plate. The electromagnetic exciter has been placed on top, though it was applied to the bottom plate of $2\cdot91$ mm thick plywood. Not my finest piece of woodwork!
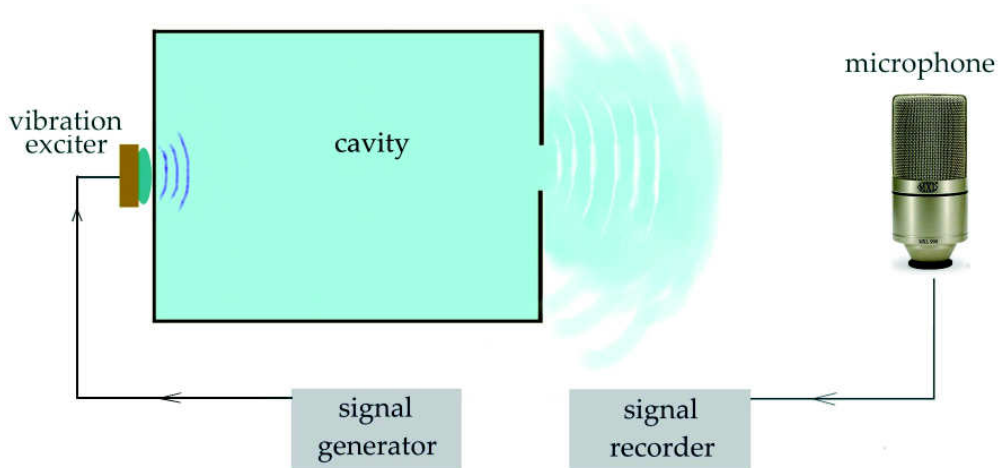

Figure 2: External microphone records sound radiated from box or violin when the wooden structure is driven by an electromagnetic vibrator.

to minimise sound leakage from back to front. The high quality capacitance audio microphone was placed about 30 cm above the aperture in the box's top, and the signal recorded as the vibrator was driven with either a steady sinusoidal vibration, or else a linearly swept sine wave.

Figure 3 shows the envelope of amplitude recorded by the microphone as the frequency sweeps slowly from 50 to 1200 Hz. The linearly swept frequency means that the time axis is equivalent to frequency. The upper green curve is with the hole open, the lower inverted yellow curve with it closed by covering it with a block of MDF. This did not make an air tight seal, but overlapped the MDF cut-out by about 3 cm. Each such recording was subsequently played through the WaveSpectra or NCH WavePad Fourier spectrum analysis software to determine the frequencies at the peaks in amplitude. The accuracy of this is about ±5 Hz, the uncertainty arising from the width of time window over which the digital Fourier transform is performed. The precision of some peaks was

refined to ±1 Hz in a further measurement in which a continuous sine wave was stepped through the resonance, 1 Hz at a time, under manual control. Here are a few observations:

1. Nominally there should be no sound with the hole closed. The sound recorded must come from leakage from the back plate through the cushions and/or from leakage around the MDF covering block.

2. By and large the sound level with the aperture closed is significantly less than with the hole open. So, to answer our opening question, Yes, the hole does let out the sound from the back plate.

3. There is a range between about 700 and 800 Hz where the sound is very low, but is louder with the hole closed. Very odd!

4. The Open curve has a large peak at 156 Hz completely absent from the Closed curve. This is the Helmholtz resonance, A0.

5. The Open curve also has a broad peak at about 410 Hz which is also absent from the Closed curve.

6. The Open curve has another narrow major peak at 1040 Hz. This is mirrored in the Closed curve but moved slightly to lower frequency. Closing the hole has not completely extinguished it.

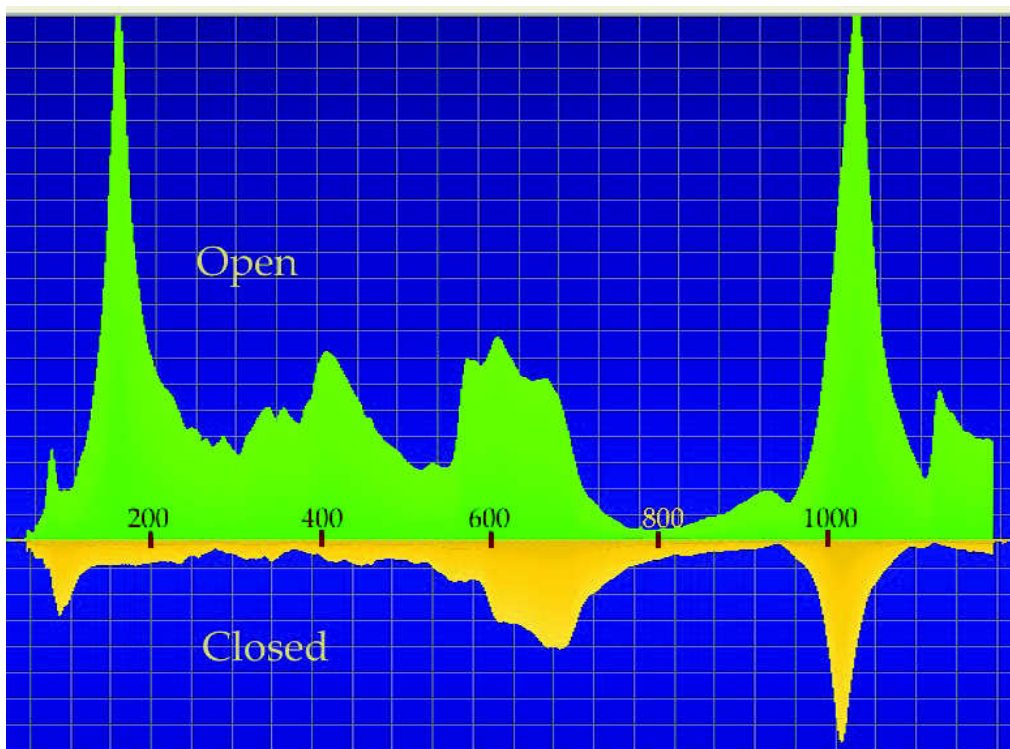7. Both curves have a broad peak between about 550 and 700 Hz.

Figure 3: Signal received at external microphone when flexible back plate of rectangular box is excited at frequencies from 50 to 1200 Hz, with the 14 mm wide hole in the top plate either open or closed. (The Closed graph is inverted.)

On the premise that measuring the amplitude-frequency response under different conditions of the air cavity might give some clues as to the functioning of the cavity and aperture, I carried out a second set of measurements on Box C with the 14 mm wide aperture. I removing all the cushions except the one supporting the box, leaving everything else as it was. With the cushions removed we hear more sound direct from the flexible back plate where the driving force is applied. The cavity was changed in turn by covering it with the MDF block, sealing it with modelling clay (Plasticine) and filling the box with light polystyrene balls ('bean bag filling'). The four amplitude-frequency curves in Figure 4 were collected with the same driving amplitude and same microphone gain so as to be directly comparable.

1. The A0 resonance at 156 Hz is suppressed by any method of closing the hole.

2. The modelling clay would give the closest seal, so the spike at about 680 Hz in the second green curve, for the MDF block covering the hole, must be to do with air leaking from under the block. Similar peaks are seen in the two curves on the left.

3. The large wide peak centred at 920 Hz when the cavity is filled with polystyrene balls has no counterpart in the other three curves, so must be something to do with modifying the resonances and/or transmission of sound through the box. The balls are so light that they are most unlikely to apply any constraint directly onto the back plate.

The third set of measurements explored further the effect of filling the cavity with polystyrene balls. I also enlarged the aperture to about double its width and recorded the curves in Figure 5 on the same scale while I filled the cavity in stages with the balls. The second off bottom curve is for the cavity full to capacity but the aperture otherwise unobstructed. The bottom curve is for the box
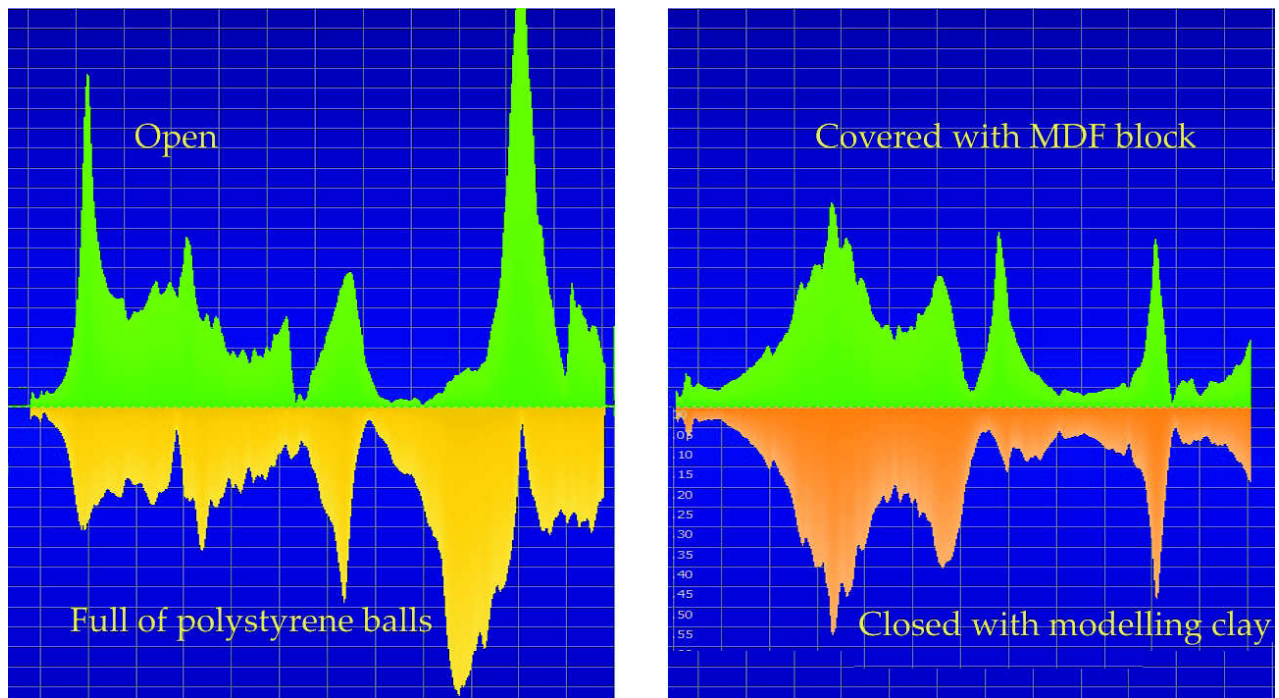

Figure 4: Four amplitude-frequency spectra, 50 to 1200 Hz, recorded under the same conditions, showing the effect of closing the air cavity by covering the 14 mm wide aperture with a wooden block, sealing it with modelling clay, and filling the cavity with small polystyrene balls. Orange curves are inverted.

full of polystyrene and the aperture tightly covered with a plug of modelling clay. Again let us note the salient points without yet trying to explain them:

1. Widening the hole has moved the A0 Helmholtz resonance to 180 or 181 Hz. It gradually dies in amplitude as the air is displaced from the cavity.

2. Similarly the peak at 573 Hz, the left of two twins in the top panel of Figure 5, fades away as the box is filled.

3. However, the right twin peak, at 685 Hz, persists so long as the aperture is open.

4. The large peak at 1040 Hz (top panel) persists in a modified state as the cavity is filled; it broadens and moves to lower frequencies.
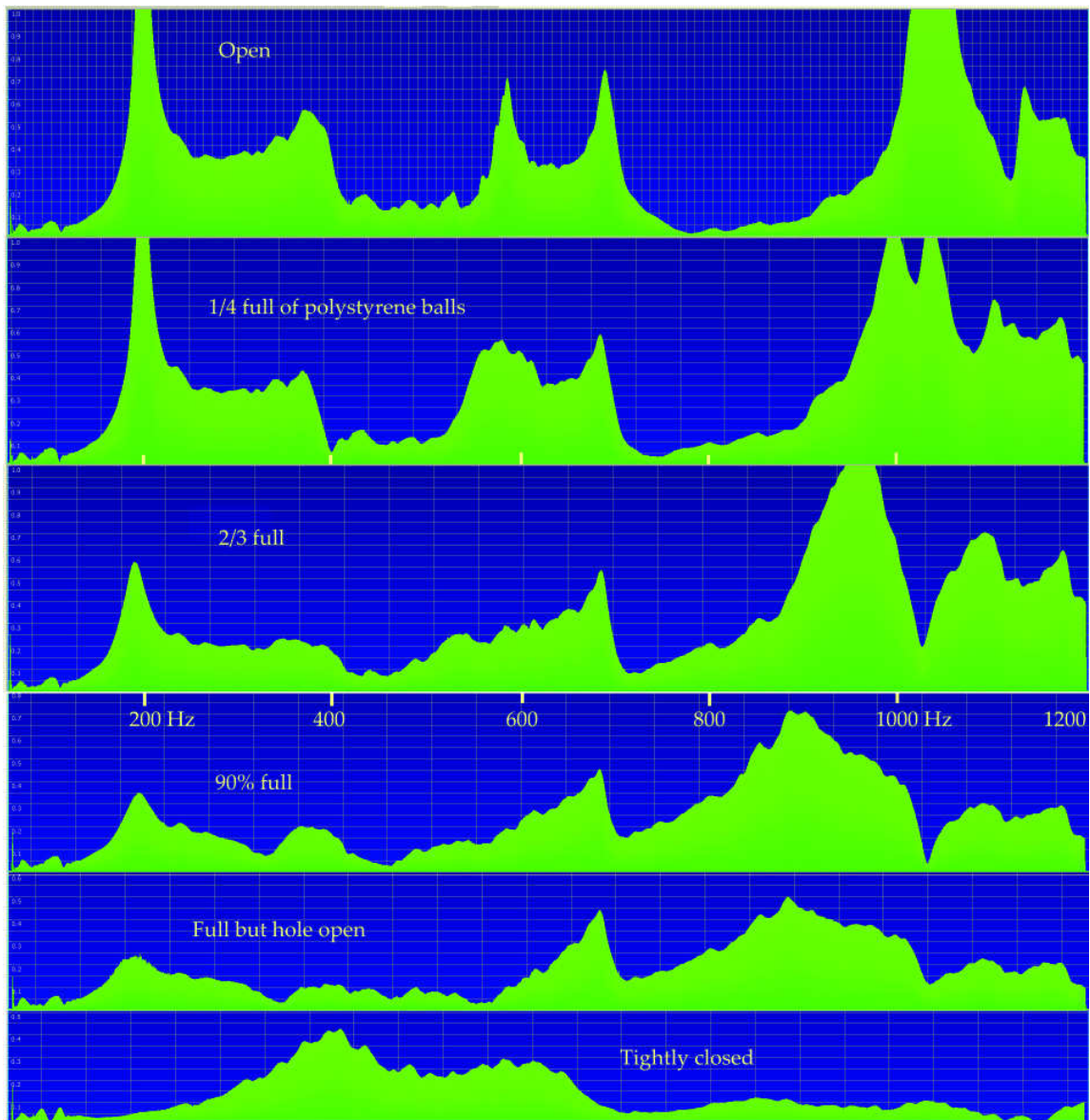

Figure 5: Amplitude received at external microphone over range 50 -1200 Hz from box increasingly filled with polystyrene balls then capped tight closed. Enlarged aperture 61 by 28 mm.

5. The smaller peak at 1130 Hz does much the same.

6. Completely sealing the hole quietens frequencies above about 700 Hz, but has the strange effect of making the sounds louder from 300 to 700 Hz. Very odd!

So here in Figures 3, 4 and 5 we have a wide view of the phenomena, giving us plenty to think about.

2.2   Elementary acoustic characteristics of the box

I am not going to try to explain all the features of Figures 3, 4 and 5 in this article. However, to orient ourselves, let us note some elementary properties of Box C with its two sizes of aperture.

I used the LISA finite element program to model the normal modes of the air cavity when it is fully closed (no aperture). LISA has the facility to solve Helmholtz's equation as explained in §6.2. Using a velocity of sound of $341 \cdot 5$ m/sec the predicted natural frequencies are at (Hz)

$$502, \quad 1005, \quad 1068, \quad 1180, \quad 1467, \quad 1508, \quad 1848. \tag{1}$$

These are readily understood as standing wave modes as follows. Let a be the long dimension of the box and b its width. The listed frequencies correspond to the following ratios of wavelength λ to box dimension:

$$a = \frac{\lambda}{2}, \quad a = \lambda, \quad b = \frac{\lambda}{2}, \quad a = \frac{\lambda}{2} \ \& \ b = \frac{\lambda}{2}, \quad a = \lambda \ \& \ b = \frac{\lambda}{2}, \quad a = \frac{3\lambda}{2}, \quad a = \frac{3\lambda}{2} \ \& \ b = \frac{\lambda}{2}.$$

To match these predictions with experiment I set up the arrangement in Figure 6. A 6 mm diameter electret microphone on two fine wires was placed inside the cavity through a small hole in the side of the box, and sealed. The microphone's output was input to a computer and digitised via the sound card at $44 \cdot 1$ kHz (CD quality) using the GoldWave signal recording software. The system was driven by a digitised pure sine wave from an NCH digital tone generator, amplified by a hi-fi amplifier and fed to a loud speaker positioned about 150 mm in front on the cavity. By this arrangement the loudspeaker forced vibrations in the air at the cavity's opening. The tone generator provided a sinusoidal wave which was ramped linearly in pitch between 50 and 1200 Hz.
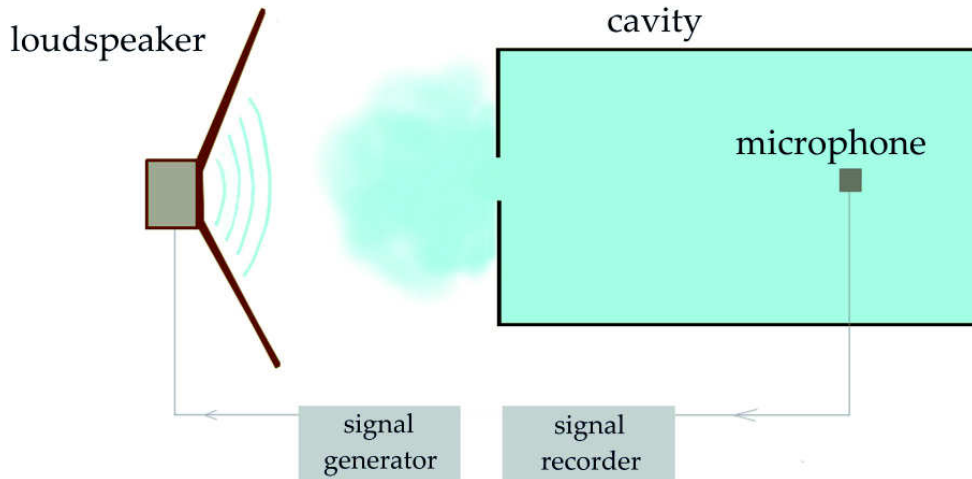

Figure 6: Arrangement for measurement of Helmholtz and higher air resonances of a cavity.

Figure 7 shows two spectra obtained once the aperture had been widened to 28 mm. They correspond to two positions of the internal microphone. Though the amplitude varies with air pressure across the cavity, these peaks remain at the same frequencies. The main ones are at

$$181, \quad 354, \quad 394, \quad 573, \quad 1053, \quad 1135 \text{ Hz.}$$

573 and 1132 are almost in the ratio 1:2 and probably can be matched to 502 and 1005 Hz at Eq 1 above, with the increase in pitch being due in some way to the aperture.

Mode	Constraint	
	z displ	no rotation
0-0	155	328
1-0	258	440
2-0	468	667
0-1	551	843
1-1	617	918
2-1	769	1079
3-0	776	1000
3-1	1027	1348

Table 1: LISA finite element predictions of modal frequencies in Hz of plywood plate 340 by 160 mm under two types of edge constraint.

To complement the above air resonances, I used the LISA FEA program also to calculate the resonances of the plywood back plate. As shown in the immediately preceding article on www.mathstudio.co.uk, the resonant frequencies depend strongly on the degree of constraint. Table 1 lists the predicted modal frequencies under two edge constraints. The one labelled 'z displ' means that every point along the perimeter is constrained not to move out of the plane of the plate, but rotation is allowed. The 'no rotation' column means that, in addition, rotation with the local edge as axis was prevented; this is the built-in condition. You can see a great difference in frequencies. The bottom plate overlapped the MDF sides and was pinned and glued all round to the MDF, so the frequencies should be close to the right-hand column.
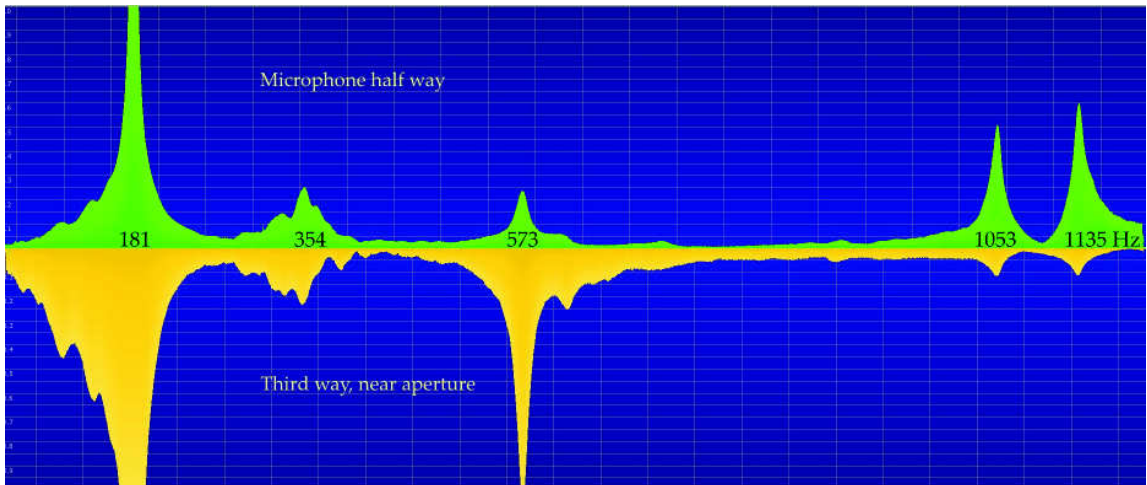

Figure 7: Amplitude received by internal microphone in arrangement of Figure 5 for Box C with enlarged (28 mm wide) aperture over range 50 to 1200 Hz. Upper panel (green) : microphone near centre of box. Lower inverted panel (orange): microphone near aperture.
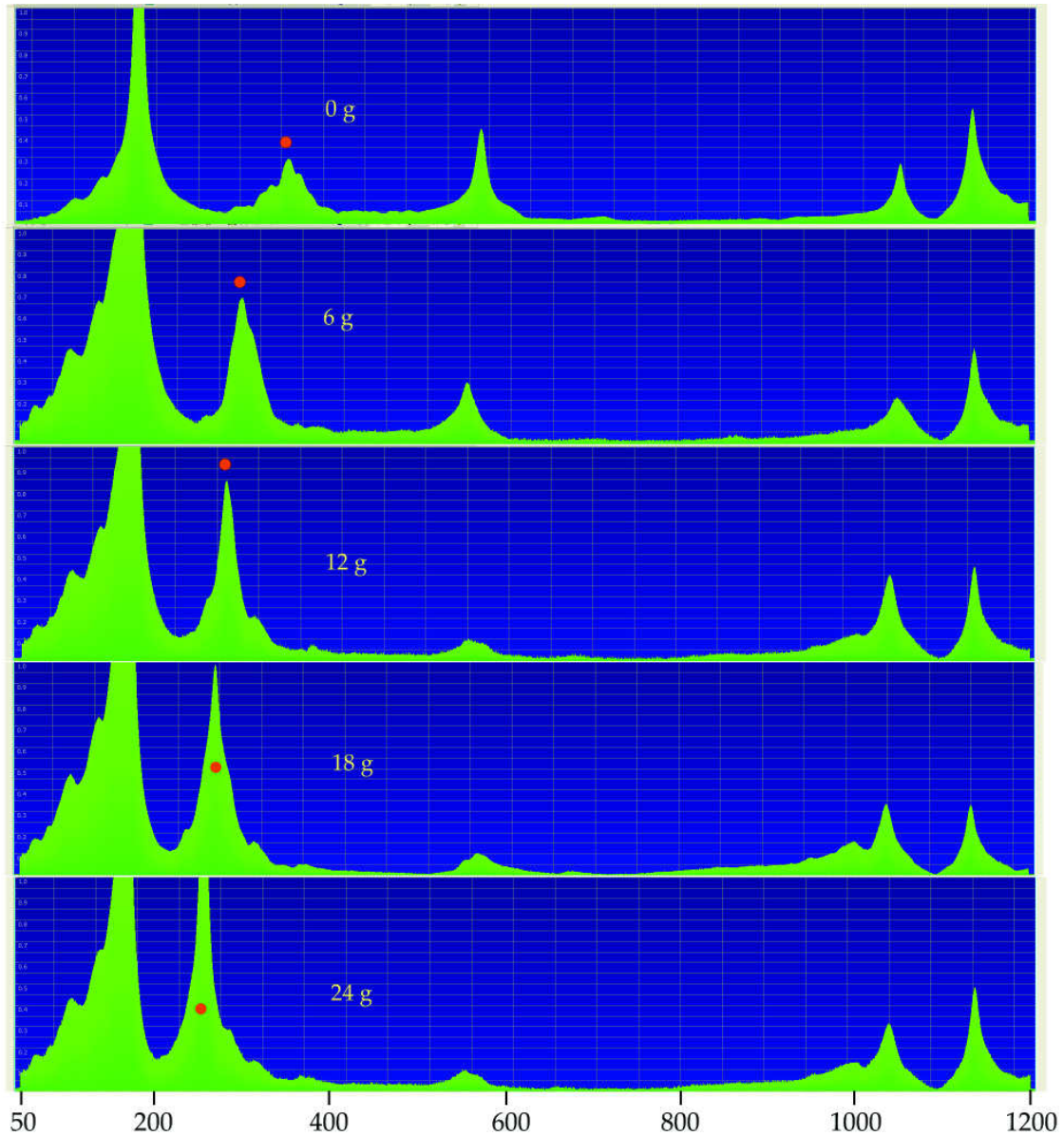
Figure 8: Five spectra showing the effect of adding mass to the centre of the flexible back plate. Signal detected by internal microphone. Aperture 61 by 28 mm.

One way to persuade the resonances to reveal whether they are primarily wood- or air-related is to add a small mass to the plate. Extra mass will lower the frequency, and this can be seen in Figure 8 where the added masses are 0, 6, 12, 18 and 24 grams respectively. The peak marked with the red spot moves to lower frequencies with added mass, so this must be a wood resonance. With no weight it is at 354 Hz, so tentatively may be matched with the 328 Hz predicted by LISA using the elastic constants of 3-ply determined in my previous article. By implication, the other resonances are air-dominated. The two observed at 1053 and 1135 Hz may tentatively be matched with the FEA predictions of 1005 and 1068 Hz in Eq 1 for a closed cavity.

That is a sufficient overview of the acoustic behaviour of this simplified box-with-hole model of a violin. We move on to direct experimental evidence for Helmholtz resonances in the actual violins and violas.

3 Experimental observations of Helmholtz resonance in violins

The A0 Helmholtz resonance can be examined in practice from two aspects:

- whether it can be excited by vibrations applied from the surrounding air,

- whether it can be excited by vibrations applied at the violin bridge.

This section deals with each of these in turn. The second mode of excitation requires effective coupling between the wooden violin belly and the air inside as we saw in Figure 3, 4 and 5.

3.1 Air cavity resonance stimulated by loudspeaker

While I readily obtain a single musical note by blowing across the neck of an empty wine or beer bottle, I have had no success in coaxing any musical note from a violin or viola by blowing across an f-hole, whether by mouth on from a hair dryer. Naively I would expect that if an f-hole can affect the sound radiated from a violin, by reciprocity one should be able to excite the f-hole resonance by a stream of air directed at it, but that seems not to be the case.

I have therefore adopted a direct means of measuring cavity resonances using the equipment in Figure 6. With a wine bottle the electret microphone was placed through the neck, and with a violin or viola through one of the f-holes

Three examples of recorded response are shown in Figure 9 for a) a wine bottle, b) a violin and c) a viola. In each case the horizontal axis is time, proportional to frequency, and the vertical axis is the unrectified amplitude. The bottle shows only one resonance, whilst the violin and viola have a strong low frequency resonance plus a weaker one at about twice the frequency, and some further response at about 1 kHz. As in §2 each such recording was subsequently played through the WaveSpectra or NCH WavePad Fourier spectrum analysis software to determine the frequencies at the peaks in amplitude to a precision of about ±5 Hz. Precision was refined to ±1 Hz in a further measurement in which a continuous sine wave was stepped manually through the resonance, 1 Hz at a time. The measured peak frequency did not depend on the position of the microphone – various positions were used. Checks with the box removed and the microphone in front of the speaker confirmed that the response of the measuring system was essentially low and flat over the whole range, so the resonance does indeed represent a major strengthening of the cavity's air vibrations.

The bottle tone is at 112 or 113 Hz, precisely the note obtained by blowing across the neck as recorded in a separate experiment with an external high quality condenser microphone. This correspondence confirms that the arrangement of Figure 6 does indeed detect the Helmholtz resonance. Note the simple, smooth shape of the peak, slightly skewed to higher frequencies. The sharpness of the resonance as measured by the full width at half height (FWHH) is about 6 Hz, or 5% of the peak value. The measured peak frequency did not depend on the position of the microphone – various positions were used.

Two violins were tested. Because the design of violins is standardised, even to the size and shape of the f-holes, their resonances were at almost the same frequencies. With a cheap factory-made Chinese Stentor violin the resonances in Hz, measured by spectrum analysis to (±5 Hz), were

$A0 = 267$ (Middle C), $A1 = 474$ (B♭), higher ones at 552, 724, 1092, 1135, 1152.

The identification of A1 is provisional, though as in §2.2 I tested to see if adding a Plasticine weight to either the top or back plate caused the frequency to drop, but it remained constant, suggesting
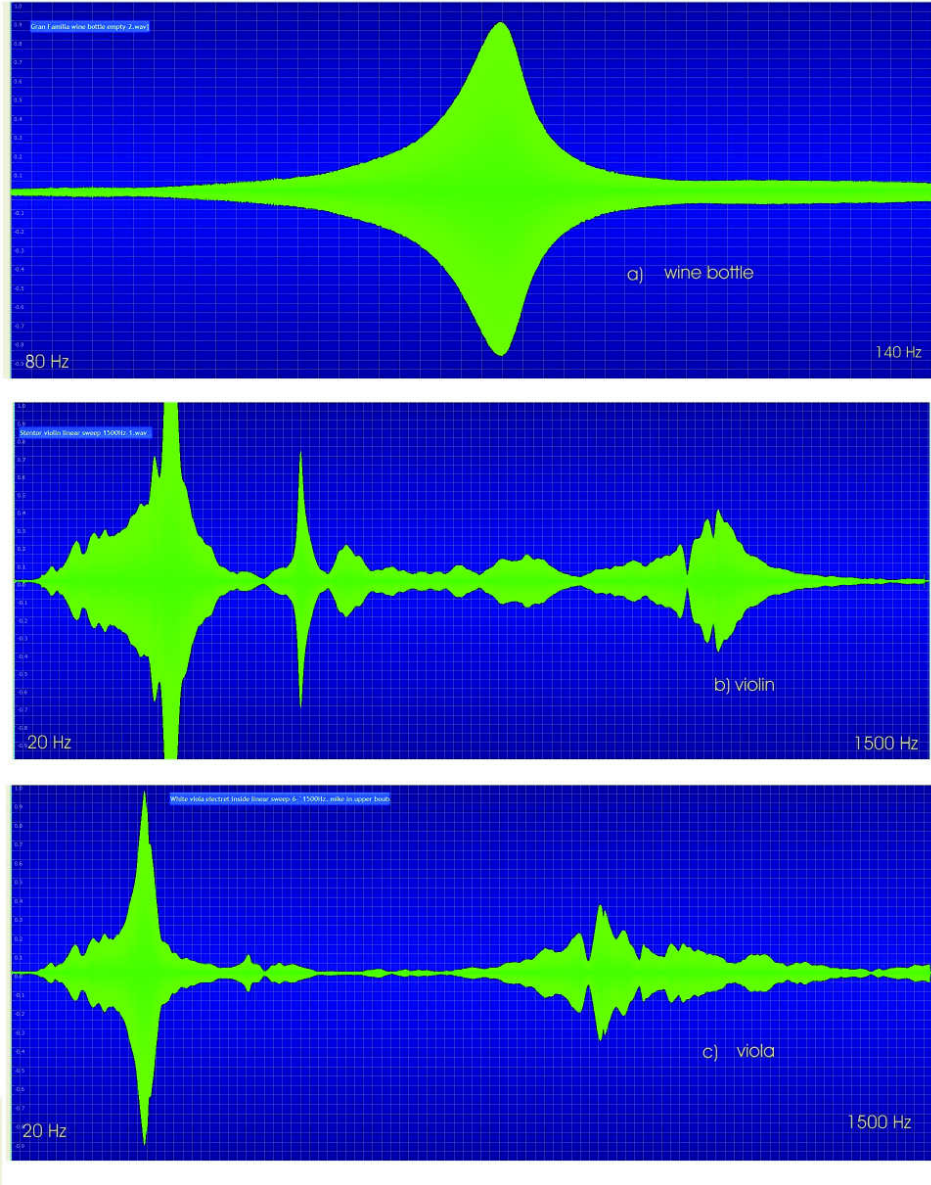
Figure 9: Frequency-amplitude spectra for a) wine bottle, b) violin and c) $16\frac{1}{2}$ inch viola, recorded with an internal microphone in the arrangement of Figure 6.

air resonances. A better quality, hand-finished Chinese violin has A0 = 270, A1 = 471 Hz. The peak is more highly skewed than for the wine bottle, and is decorated on its low frequency shoulder with several smaller peaks. These *may* be associated with the flexibility of the walls and their rectangular shape, but that is mere conjecture. Similar decoration with subsidiary peaks was found with Box C – see Figures 7 and 8. The FWHH of the A0 peak is 28 Hz, from 249 to 277 Hz, 11% of the resonance centre frequency and about ±1 semitone (B to C♯).

When the f-hole near the E string was fully covered with a strip of card and masking tape, the A0 resonance dropped to 198 Hz (low G), 75% of its open value, but the A1 resonance remained essentially unchanged at 466 Hz. This supports the view that the A0 and A1 resonances are different in kind, the former depending on the f-hole openings and the latter only on the cavity itself. A1

11

Instrument	both open	upper open lower $\frac{1}{2}$ closed	upper open lower closed	upper closed lower open	upper closed lower $\frac{1}{2}$ closed
14 inch violin	271	235	200	196	140
$15\frac{1}{2}$ viola	244			198	
$16\frac{1}{4}$ viola	220		163		
$16\frac{1}{2}$ viola	228		174	163	
Tertis viola	208		153		
JMC Plywood	107				

Table 2: The A0 Helmholtz frequency in Hz of a violin and five violas with the f-holes with various degrees of occlusion. The upper f-hole for a violin is near the E string, etc.

and higher air modes are probably similar to standing wavers in organ pipes, where the frequency is determined by the cavity length equalling half a wavelength. The velocity of sound in air at room temperature is $341 \cdot 5$ m/sec. Therefore if half a wavelength fits into the cavity at about 470 Hz, the cavity's length is $36 \cdot 3$ cm, which is almost exactly the length of a 14 inch violin.

The air resonance frequencies of a $16\frac{1}{2}$ inch viola were (± 5 Hz)

$$A0 = 224 \text{ (low A)}, \quad A1 = 390 \text{ (G)}, \quad \text{higher ones at } 455, \ 950, \ 995 \text{ Hz.}$$

Again A1 corresponds to half a wavelength fitting into a length of 44 cm, or 17 inches. In Figure 9c A1 is weak, but its strength depends on where the microphone is placed, as one would expect for an organ pipe mode. The A1 signal should be strongest near the centre of the instrument.

The 1 Hz stepped continuous wave technique was used to measure A0 more precisely for several instruments, with the f-holes variously open or closed. Results are listed in Table 2. The upper f-hole is near the E string on a violin and near the A on a viola, and similarly the lower is near the G or C string respectively. The 'JMC plywood' viola is the large, asymmetric, non-standard instrument made by the author at the start of these acoustic investigations, as described in the companion article 'A reconsideration of the construction and acoustics of the viola'. The first column of numbers shows that as the belly of the instrument becomes larger, A0 drops. Covering one f-hole drops A0 on average to 75%, down a musical fourth. As expected, it matters little which hole is blanked off. With the violin the G hole was also half covered to leave only the central 32 mm open. The top row therefore records a reducing aperture, from 2 holes open to only $\frac{1}{2}$ a hole, in half-hole steps. It is therefore possible to tune A0 downwards by partially covering the f-holes, though the amplitude decreases as the hole is covered.

3.2 Excitation of A0 resonance from the violin bridge

The measurements described in this subsection were performed using the arrangement in Figure 2. Excitation was from the electromagnetic acoustic exciter, shown in Figure 1, held against the violin or viola bridge. This assesses all the links in the acoustic chain from excitation of the bridge, transfer to the top plate, vibration of the whole box structure, coupling to the air, and combined radiation from the wooden plates and f-holes.

The electromagnetic exciter was capped with a pad of balsa wood and held steady, by hand, against the top corner of the bridge so that most of the displacement was along the bowing direction. In most cases it was held at the E-string edge of the bridge; I did check whether is made much
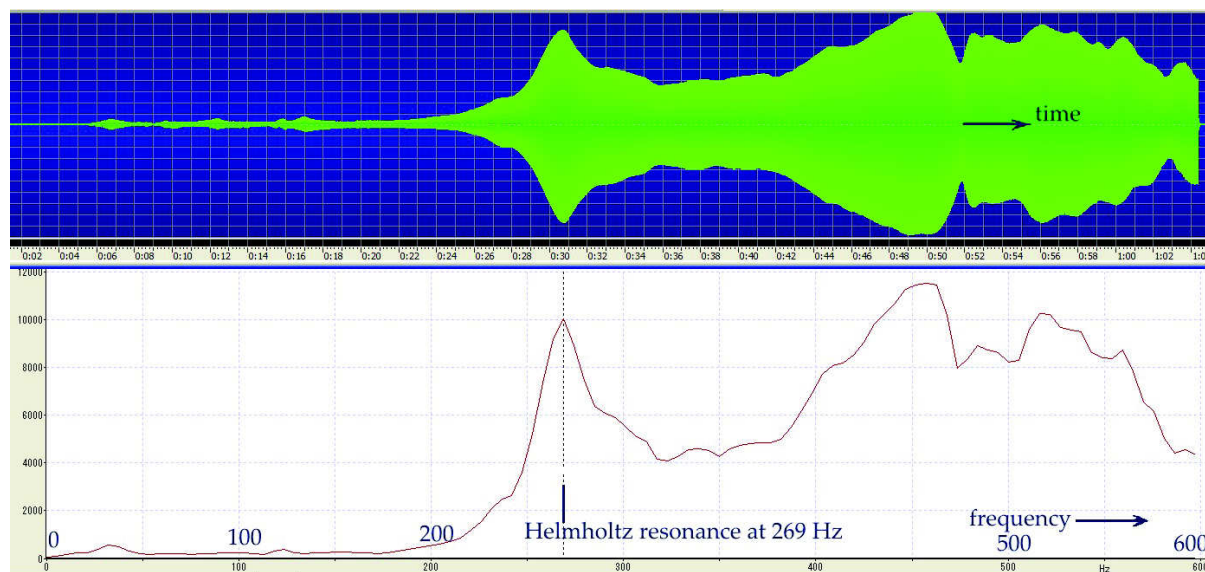
Figure 10: Radiated sound spectrum from a violin excited by sinusoidal vibrations applied to the bridge. Top panel: waveform recorded in GoldWave as frequency is swept in linear ramp. Lower panel: cumulative spectral peak value in WaveSpectra.
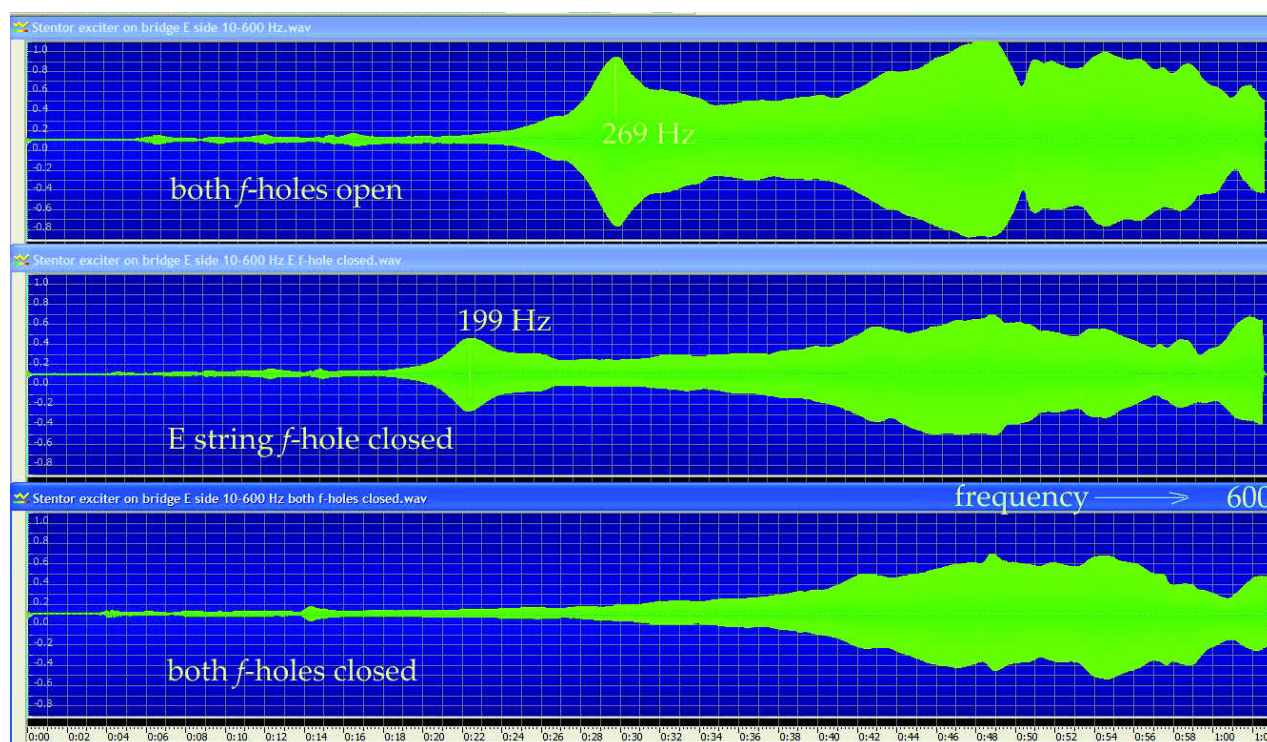
Figure 11: Swept frequency radiated sound of violin, 0 to 600 Hz, with 0, 1 and 2 f-holes closed.

difference if placed at the G string end, but it didn't. The waveform was again sinusoidal – not the saw tooth applied by a moving bow, but in principle more simple to understand. The microphone was a high quality condenser type positioned half a metre above the violin. The strings were again damped with sponge pads and the instrument held by the neck as in normal play.

13

Figure 12: Swept frequency radiated sound from $16\frac{1}{2}$ inch viola, 0 to 600 Hz, showing effect of closing one or both f-holes.
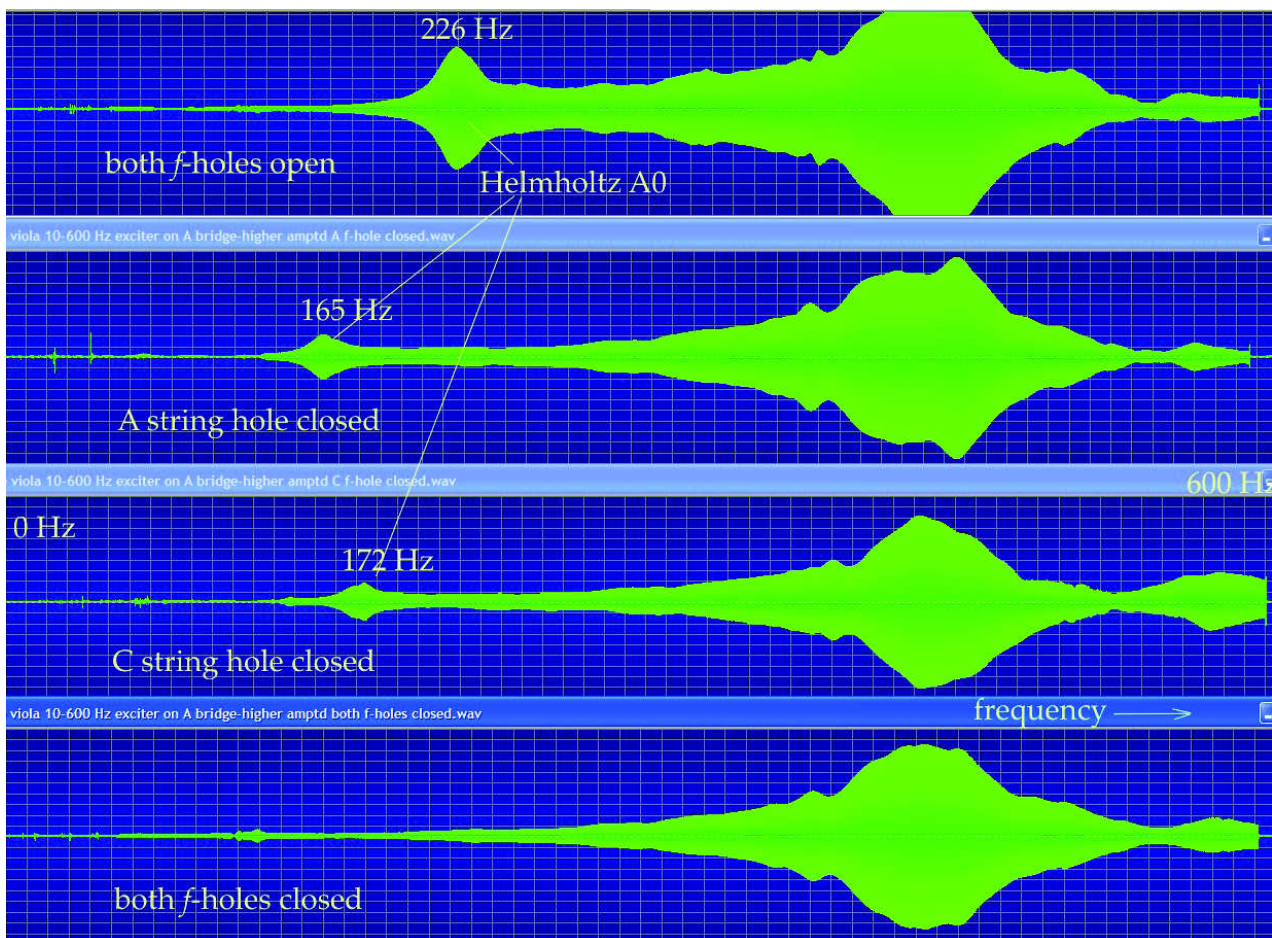
Figure 10 shows the response in two formats. The top panel is the full unrectified wave recorded as time progresses in the GoldWave software, as in Figure 9. The range is from near zero to 600 Hz. The lower panel is from the WaveSpectra program. This sweeps a window along the recorded sound clip, taking a digital Fourier transform as it goes. The largest amplitude at each frequency is plotted and matches well with the raw waveform above.

Figure 11 and 12 respectively show the effects of closing the f-holes in a violin and a viola. You can see the Helmholtz resonance and how it moves to lower frequency and lower amplitude as one f-hole is covered. Closing both holes dampens A0 totally. The frequency of A0, measured with WaveSpectra to about ±5 Hz, agree with the values determined using loudspeaker excitation and the internal microphone, and listed in Table 2. I confirmed this on three violins and four violas.

I did not make a determined effort to measure the amplitude of the sound radiated at A0, but it does fall if one f-hole is covered. In one test both f-holes were initially covered with card and the acoustic exciter held by one person against the bridge while a second person carefully uncovered one f-hole then both. This was done with continuous wave excitation at 440 Hz, where the violin has a large response. The amplitude of this sound remained virtually unchanged as the holes were uncovered. This means that the large stable peak near 440 Hz can serve as a reference for amplitude. The amplitude of A0 relative to this reference peak is in the range from about 90% to 110% and this

14

drops to about 50% to 65% for a violin when one f-hole is covered. For a large viola it falls from about 50-60% to about 20-25%. Roughly, therefore, the amplitude falls to about half, roughly equal to the decrease in area when one hole is covered.

I carried out a limited series of tests actually bowing the instrument. Much as in the 'loudness curves' of Hutchins and Saunders to be described in the next section, I played either a chromatic scale or glissando slide on the instrument while recording the sound about two metres away with the hi-fi quality condenser microphone. Figure 13 shows the GoldWave wav. files for a chromatic scale bowed on a violin G string for both f-holes open, one or other closed, and both closed. It was only a cheap violin, so aurally the tone quality is not high. With both holes open (the usual case) the tone was full if rather rough. With the upper hole closed, it sounded more nasal, rather like a viola, and more strangled. Surprisingly, the tone with only the lower hole closed was better though still nasal. With both closed the sound was thin and 'boxed-in', apart from on the open G string. These are, of course, just subjective assessments, and indeed the bowing of each note could not be identical even though nominally the same *detaché* strokes were bowed. With both holes open A0 is at 271 Hz (Table 2), about C♯ above Middle C, and one can see in Figure 13 the slightly larger amplitude here. With one hole closed A0 falls to about 200 Hz, roughly the open G string. This G (first note) is indeed prominent in the middle two panels and we might be led to ascribed this to A0 were it not that the same G is strong also in the bottom panel where A0 has disappeared. So the louder sound
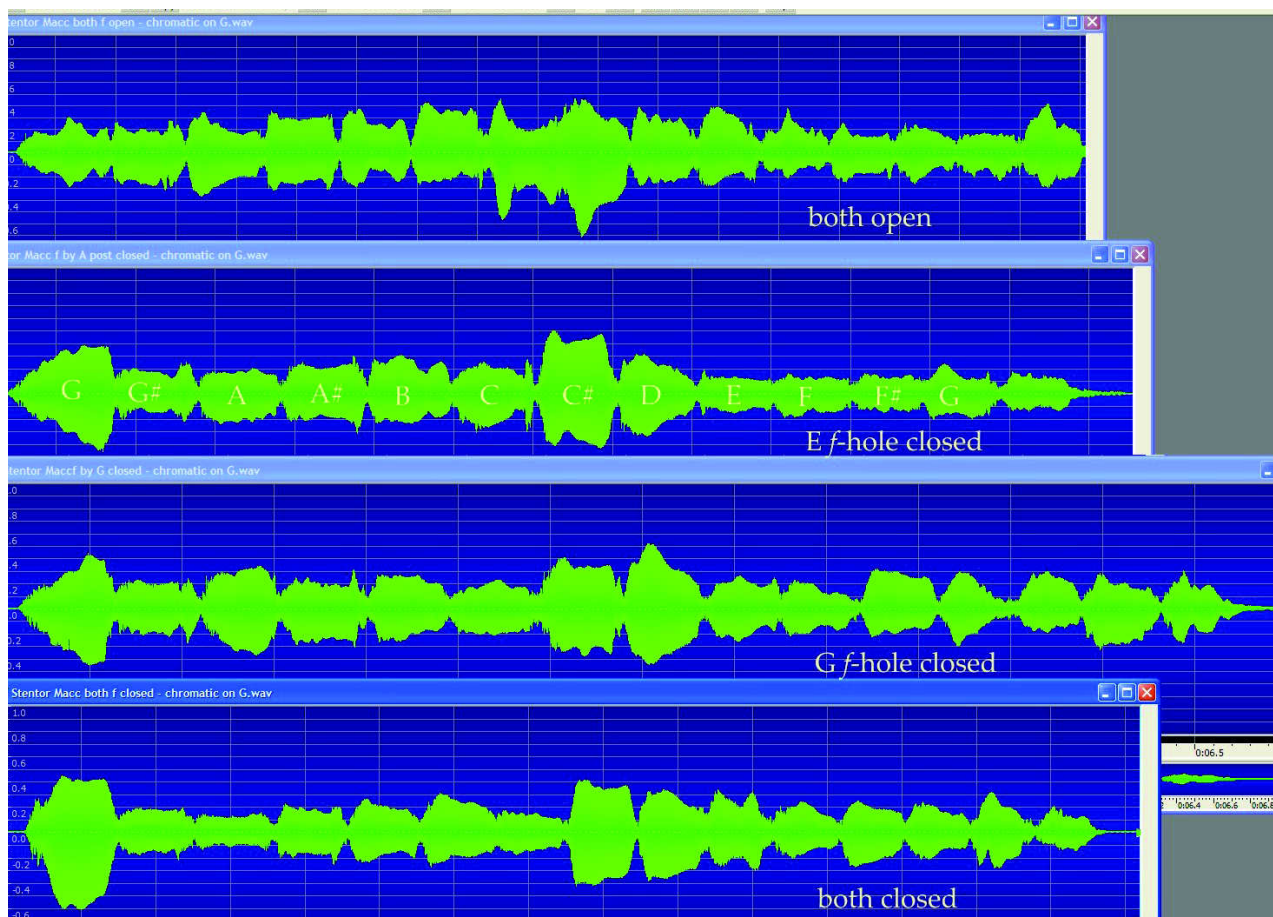

Figure 13: Waveforms as a chromatic scale is played by bowing a violin on the G string under four conditions of the f-holes.

15

here is probably more to do with it being an open string [2]. Moreover, a strong response at C♯ is clear in the lower three panels, even though A0 is no longer at C♯ in these three cases. So, though there is some aural effect of A0, this short exploration is far from conclusive.

This section has presented conclusive evidence for the existence of the Helmholtz and higher air cavity resonances of a violin and viola, and also shown that A0 can be excited by lateral motion of the bridge, as produced by the bow in playing. The effects on perceived tonal quality while playing the violin with a bow, however, need further investigation. We therefore look in the next section at some of the older pioneering literature on how the air resonances and f-holes are thought to affect the tonal quality of an instrument.

4   Published literature on the musical significance of A0

Firm statements about the air and main wood resonances have been made by the USA pioneers Carleen Hutchins and Frederick Saunders in papers republished in 'Musical Acoustics, Part I: Violin Family Components'[3]. Hutchins was a founder of the Catgut Acoustical Society of America. Many papers on violin acoustics have been published in its journal, though at the time of writing they are not available on the internet, nor does my local university library subscribe. There must be a wealth of information there which most people cannot access.

To understand Hutchin's terminology, refer back to Figure 8 of §2 which shows spectra for Box C. A0 is the Helmholtz resonance at 181 Hz, A1 the higher air resonance at 572 Hz and the peak at 354 Hz, which moves to lower frequency when mass is added, is the 'main wood resonance'. In Table 1 this is labelled 0-0 and predicted by FEA to be at 328 Hz. In previous articles I have called this the breathing mode because the whole plate flexes in and out like a diaphragm.

Hutchins, Saunders and others found the loudness curve to be a useful tool. Examples are given in Figures 14, 15 and 16. A chromatic scale is played with the bow, the player producing the loudest sound without the note breaking up. The loudness of each note is measured with a commercial loudness meter. The black dot in the figures is the main wood resonance, the white circle the A0 air resonance, and the low frequency grey circle the 'wood prime' resonance – more about that shortly. In a 1962 review paper Hutchins (page 8 *et seq.*) says

> Tests show that a good violin usually has its main wood resonance within a whole tone of 440 Hz, the note A, to which the second off highest string is tuned.

She also states

> In a good violin the main wood resonance and the main air resonance fall approximately 7 semitones, or one musical fifth, apart. In some poor instruments they can be as much as 12 semitones (one octave) apart.

The pioneers appreciated that a listener's subjective impression of the loudness of notes is more even across the frequency range than these loudness curves would suggest. This is because the ear and brain attribute to the fundamental pitch all contributions from higher harmonics, some of which may actually be stronger than the fundamental. Nevertheless, the wood prime resonance is somewhat mysterious. Hutchins says that

---

[2]A string stopped with a finger has a softer end condition than one clamped at the wooden nut, so stopped strings generally have a softer, sweeter tone than open strings.

[3]Ed. C Hutchins, published Dowden, Hutchinson and Ross inc, 1975

An octave below the main wood resonance there is almost always another strong peak of loudness – it can be called a subharmonic. If one harmonic of a complex tone is strengthened, the ear will hear an increase in loudness of the note as a whole with a slight change in quality but no change in pitch. By this process the wood peak is strengthened by the tone of the main wood resonance an octave above. The subharmonic of the main wood resonance benefits the lower tones of the violin.

Hutchins, Saunders and Hopping[4] described experiments into subharmonics which 'strengthen the lower tones of the violin which are weak because the area of the body is too small to emit natural responses in this range.' From this paper I understand that a subharmonic seems to be the sympathetic resonance at low frequency when a note corresponding in pitch to a harmonic of this low note is bowed on the violin. They give the analogy of holding down the key C an octave below middle C (to lift the damper) and then striking middle C; the vibrations from middle C stimulate the lower string and cause it to supply a weak note one octave below the note actually struck. For this principle to apply to a violin the instrument would need to have a resonance at low frequency for this to be stimulated by a note an octave higher; I cannot see this being the case, so still find the wood prime subresonance a mystery.

---

[4] J. Acoust Soc Amer. Vol 32, No 11, 1443-1449, 1960

VIOLIN "LOUDNESS CURVES" compare maximum sound levels produced at semitone intervals by a good 1713 Stradivarius (*top*), a poor 250-year-old violin of doubtful origin (*middle*) and a poorer, somewhat older instrument credited to P. Guarneri (*bottom*). Only the first shows desirable spacing and strength of wood (*black dot*), "wood prime" (*gray dot*) and air resonances (*open circle*). Letters at bottom indicate tuning of open strings.
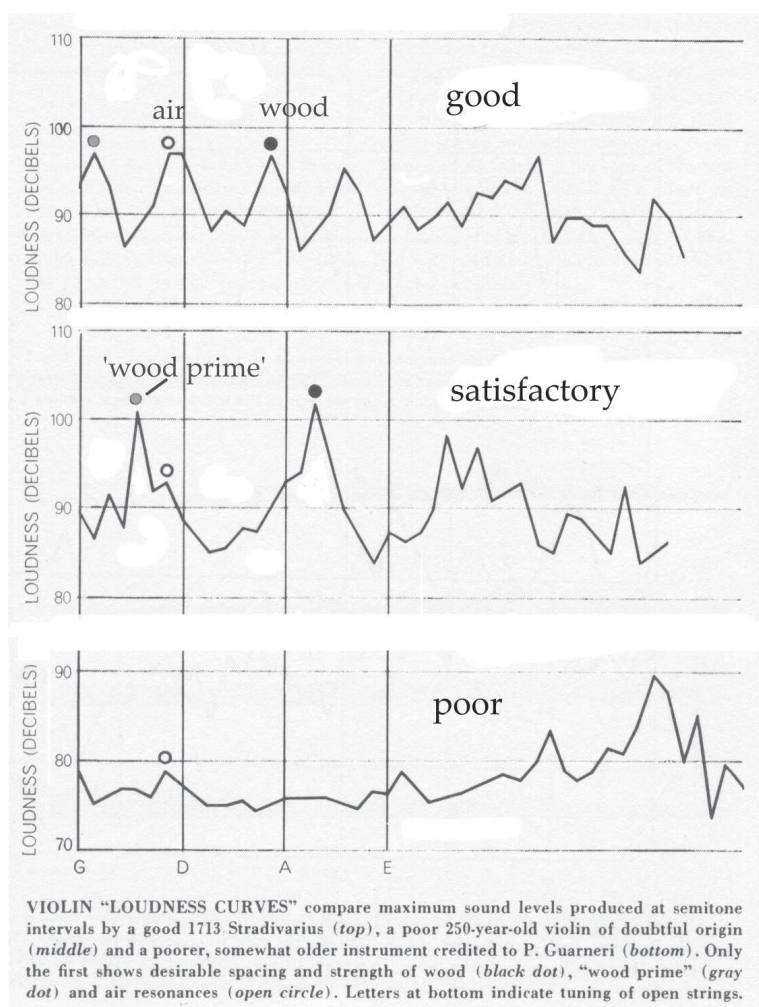
Figure 14: Loudness curves of three violins of different qualities, after Carleen Hutchins.
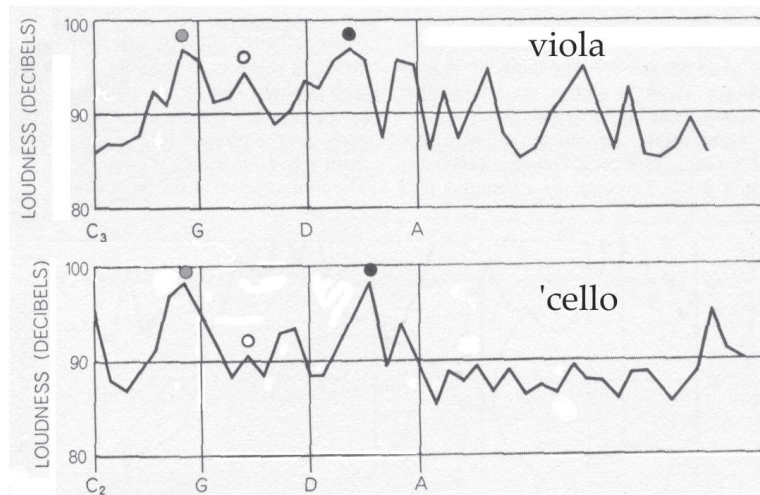
Figure 15: Loudness curves of a viola and a 'cello, after Hutchins

Hutchins also says

> Spacing the main wood and air resonances about a half-octave apart spreads these peaks
> so that the air-tone peak falls nicely in the middle of the octave between the wood
> resonance and its subharmonic. ...... In the best violins the main wood and air resonances
> invariably fall within a semitone or two of the frequency of the two open middle strings,
> the wood resonance corresponding to the higher tuned string (A on a violin). ...... This
> is not true of the viola and cello. In these the two resonances fall 3 or 4 semitones higher
> than the middle two open strings. ... The resonances are too far above the lower notes
> of the instruments and these suffer in strength and quality.

In a paper submitted in 1986, Carleen Hutchins describes comprehensive experiments to see
whether the higher air cavity resonances have an effect on the tone quality of violins [5] She drilled
dozens of holes through the ribs to puncture the air cavity, exploring the effects of plugging some
of these with cork or foam. She also buried this 'Swiss cheese' violin in sand to dampen the wood
modes, and concluded that

> There is a marked decrease in tone quality, especially in the lower octaves, when the
> amplitudes of the cavity modes are greatly reduced by either 1) opening a series of
> small holes all around the ribs, which shifts the frequencies of these modes up the scale
> away from the lower octave: or 2) damping the high-Q cavity modes in this range with
> foam plugs inserted in the rib holes, which also shifts the mode frequencies up the scale.
> These findings show the existence of strong interactions between the resonances of the
> mechanical structure of the violin and some of its cavity modes, and indicate that these
> interactions are musically significant.

Another noteworthy book is 'The Physics of the Violin' by Lothar Cremer[6]. This has much
worthy discussion and analysis of physics, though perhaps does not address the key issues in a way
which would assist a violin maker or technician. Cremer (p 253) confirms that the f−hole resonance
lies near the open D string on a violin 'and may be found by sliding the finger up and down the
lowest (G) string. ... If one f−hole is covered with adhesive tape, the resonance is lowered by a
tritone, to A flat.' My measurements in §2 clearly show flattening by a further semitone.

---

[5] J. Acoustic Soc America, vol 87, 392-397, 1990.
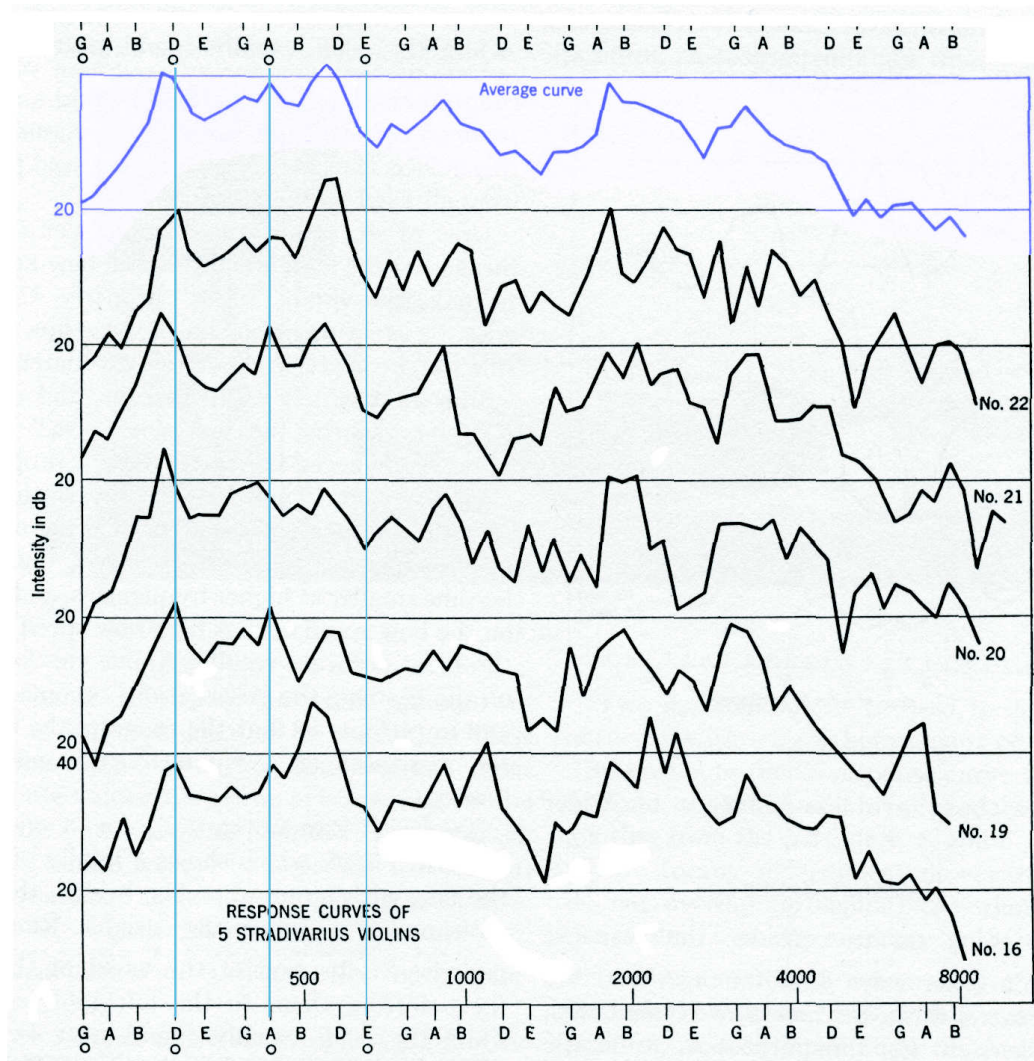[6] 1981, translated into English and published 1984 by MIT Press.

Figure 16: Loudness curves for 5 Stradivarius violins, after Saunders, 1937.

George Bissinger is another who has published much on violin acoustics. He advocates A0 as one of five 'signature modes' of a violin[7] which are purported to be sufficient to characterise the tonal quality of an instrument. Two are A0 and A1, which Bissinger says are coupled to each other (though I do not know what he means by this). The other three signatures are modes of the violin belly, which he calls the corpus, being the top and back plates plus the ribs. One mode, called C2 or CBR ('centre bout rhomboid'), is said to have shear-like in-plane relative motion of the top and back plates. The other two, called B1+ and B1−, involve the wood to one side of an f-hole moving (transverse to the plate surface) in the opposite direction to that on the other side. According to Bissinger B1+ and B1− radiate strongly directly from the wood and also because they pump air at the f-holes.

Bissinger states that strongly radiating A0, B1+ and B1− modes over the pitch range of the open strings on a violin (196 to 660 Hz) are crucial for the sound. However, he finds that all violins, excellent and poor alike, measure similarly over these five signature modes and other physical

---

[7]e.g. G. Bissinger, J. Acoust. Soc. Am. Vol 124, 1764-1773 (2008).

properties. This means that physical measurements can identify a violin from other instruments, but do not pick the Stradivarius from the student's Stentor. The only measurements distinguishing highly prized violins was that they were more even across the frequency range and strong in the lowest register, largely due to clear radiation from the f-holes at A0.

My own reaction to these studies is one of interest but some confusion and scepticism. While I do not doubt that quality investigations have been made by these various researchers, I am puzzled by the influence attributed to A0 over a frequency range which is more than one semitone either side of its centre frequency. Are the small peaks on the low frequency shoulder of A0 (Figure 9 b, c) musically significant? Also I cannot see how A0 and A1 can be coupled except being both determined by the dimensions of the belly. Moreover, I do not understand this wood prime subresonance if it is not actually a low frequency vibrational mode of the instrument. Nevertheless, these researchers say clearly that the A0 and main wood resonance should be strong and placed in pitch close to D and A of a violin's open strings, and as close to G and D on a viola as can be achieved. We know that A0 can be tuned by changing the dimensions of the f-holes, and the wood resonance is determined by several adjustable parameters, of which I suspect the edge constraint to be probably the most important – more so that the thickness of the wood, even though the commonly held view is that the plate thicknesses are crucial. Tuning of violin plates is a topic with a wide technical literature and probably an even wider folk lore.

5 Classic theory of the Helmholtz resonator

Before deriving the classic formula for the A0 resonant frequency it is informative to consider the alternative case in which the fluid, instead of being a compressible gas, is an incompressible liquid. Picture a submersed rigid container of sectional area A_c with a narrow neck of sectional area A_n opening into an infinite external pool of liquid. Suppose also that at its opposite end the container is closed with a piston, sectional area A_c, which vibrates sinusoidally with amplitude b. The peak displacement of volume in the body of the container is $\pm A_c b$ and, because the liquid is incompressible, the same volume must alternately be ejected and sucked in through the neck. Clearly in this situation the fluid in the neck behaves as a plug moving to and fro through a magnified distance $A_c b/A_n$. On replacing the liquid with a gas, the essential difference is that the change in volume within the cavity can be effected without an externally driven piston, but instead by the elastic bulk expansion and contraction of the contained gas. In the case of a violin where the box has flexible walls vibrating with the string and bridge, some of the piston-like driving action still occurs.

5.1 Derivation

The left panel in Figure 17 shows the basic rigid resonator of volume V, and the right panel its representation as a mass m on a spring with constant S. The narrow neck to the resonator has length L and cross sectional area A. This is a low frequency mode of vibration in which changes in air pressure travel almost instantaneously through the air in the cavity, so that at any instant the pressure inside is essentially uniform. The plug of air in the neck moves periodically up and down against the cushion of air in the cavity.

Sound vibrations take place adiabatically since there is not enough time in the pressure cycle for temperatures to stabilize. For a fixed mass of perfect gas undergoing adiabatic expansion or compression, the total pressure is related to volume by
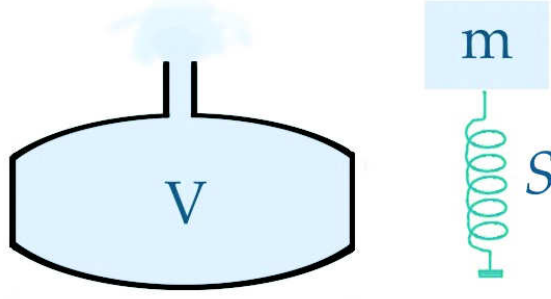
$$PV^\gamma = constant$$

Figure 17: Diagram of a Helmholtz resonator and its representation by a mass on a spring.

where $\gamma = C_p/C_v$ is the ratio of specific heats. In differential form this is

$$\frac{\delta P}{P} = -\gamma \frac{\delta V}{V}.$$

The bulk modulus K of the gas is defined by the pressure change associated with a fractional change in volume:

$$K = -\frac{\delta P}{\delta V/V} = -V\frac{\delta P}{\delta V}. \tag{2}$$

$K = \gamma P$ is also related to the velocity of sound in air,[8] c, by

$$c = \sqrt{\frac{K}{\rho}}, \qquad \rho = \text{density of air}. \tag{3}$$

Suppose the air plug is displaced a distance ξ down into the neck. This compresses the air and the out of balance force causes acceleration according to Newton's second law:

$$\text{force} = m\frac{d^2\xi}{dt^2}.$$

The volume decreases by $A\xi$ so from Eq 1 the pressure increases by

$$\delta P = K\frac{A\xi}{V}$$

and the restoring force is $KA^2\xi/V$. Since the mass of the plug is $AL\rho$, Newton's law describes simple harmonic motion:

$$-K\frac{A^2\xi}{V} = AL\rho\frac{d^2\xi}{dt^2}$$

$$\text{from which } \frac{d^2\xi}{dt^2} + \omega^2 x = 0, \qquad \omega^2 = \frac{c^2 A}{LV}. \tag{4a}$$

In hertz the resonant frequency is

$$f_{Helm} = \frac{c}{2\pi}\sqrt{\frac{A}{LV}}. \tag{4b}$$

This is the classic formula in many textbooks. It states that if the area is halved, the frequency should drop to $1/\sqrt{2} = 71\%$, or by 6 semitones. This can be applied to the f-holes of a violin since they will act as one combined mass because the pressure in the cavity is the same at each hole. The average of my measurements reported in Table 2, §2 is only a 75% drop, one semitone less.

---

[8]The fact that c does not vary with pressure is due to the density of the gas also being proportional to P.
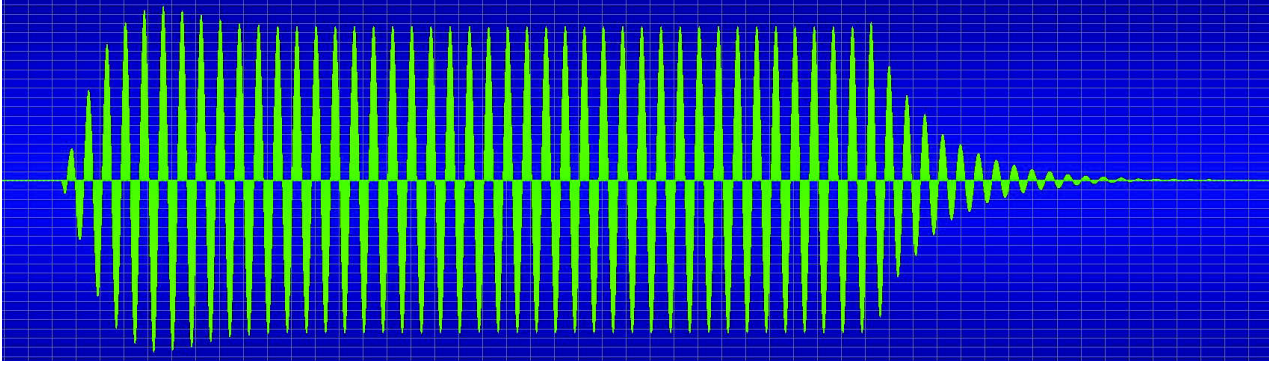
Figure 18: Response of a Helmholtz resonator driven by a tone burst of sine wave just below its resonant frequency.

5.2 Damping and Q-factor

The derivation in §5.1 is clearly only an approximation since it ignores sound radiation from the aperture plus viscous and other losses of energy which dampen the oscillations. Here I review the main features of any damped harmonic oscillator, leaving the theory particular to a Helmholtz resonator until §5.4. Essentially Newton's second law gives the equation of motion

$$M\ddot{\xi} = -S\xi - R\dot{\xi} + F$$

where M is mass, $S\xi$ a spring force, $R\dot{\xi}$ a dissipative force depending on particle velocity $\dot{\xi}$, F is an applied driving force, and the dot indicates time derivative. The solution consists of two parts:

- a particular solution fitting the given form of F, which gives the steady state behaviour while F is operating, and

- a complementary function which satisfies the equation with $F = 0$, which describes the transient when F is switched on or off.

  The complementary function is

$$\xi = \mathcal{C} \exp\left(-\frac{R}{2M}t\right) \cos\left\{t\sqrt{\frac{S}{M} - \frac{R^2}{4M^2}} + \phi\right\}. \tag{5}$$

Here $\mathcal{C}$ is an arbitrary constant representing peak amplitude and ϕ an arbitrary phase, both of which need to be chosen to match initial conditions. Two points can be noted from Eq 5:

- The displacement ξ decays exponentially, reducing to $1/e = 37\%$ of its initial value in a time $\tau = 2M/R$, and has all but disappeared in time 4τ.

- The prevailing frequency during this decay is

$$\omega_d = \sqrt{\frac{S}{M} - \frac{R^2}{4M^2}} = \sqrt{\omega_0^2 - \frac{1}{\tau^2}} = \omega_0\sqrt{1 - \frac{1}{(\omega_0\tau)^2}} \tag{6}$$

where $\omega_0 = \sqrt{(S/M)}$ is the undamped natural frequency, *i.e.* when $R = 0$. For a Helmholtz resonator ω_0 is given at Eq 4. So light damping lowers the observed frequency a little.
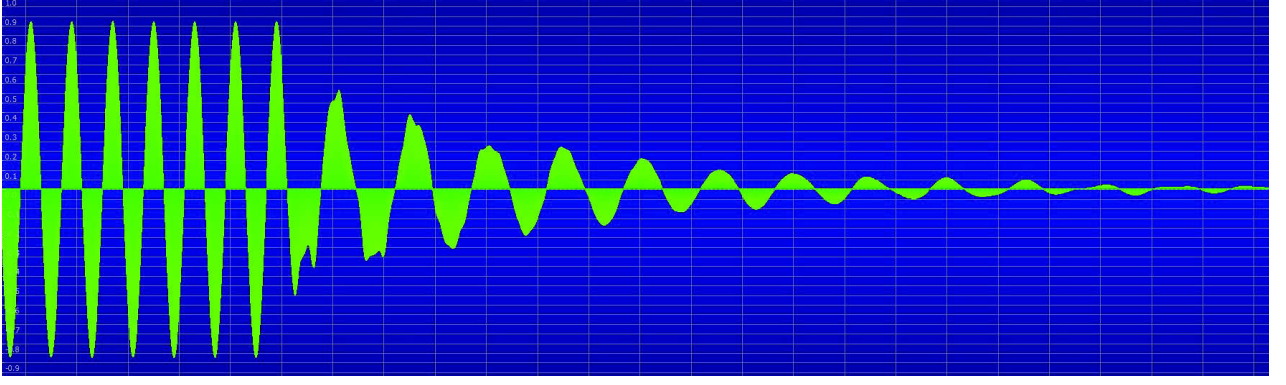
Figure 19: Decay of response after a driving tone burst at about twice the resonant frequency.

The two types of response, driven and transient, are nicely illustrated in the two wave traces in Figures 18 and 19. These show the responses recorded by a microphone when Box C (see §2) with flexible plywood back plate and smaller aperture (53 by 14 mm) is excited by a tone burst from an electro-mechanical exciter in the arrangement of Figure 2. The Helmholtz frequency, which is the natural frequency ω_0, is 134 Hz. The decaying signal has dropped to about 37% of its peak value after about $3 \cdot 4$ cycles at 134 Hz, lasting 25 ms. Figure 19 shows clearly the change in prevailing frequency when a driving oscillation at about twice resonance (250 Hz) is suddenly turned off.

Regarding the driven state, let $F = \cos \omega t$. A particular solution is found by trying possible solutions of the form $\xi = A \cos \omega t + B \sin \omega t$. The result is

$$\xi \;=\; \frac{(S - M\omega^2)\cos \omega t \;+\; R\omega \sin \omega t}{M^2 \omega^4 - (2MS - R^2)\omega^2 + S^2}. \tag{7}$$

The total displacement with F switched on is the sum of Eqs 5 and 7. However, when F has been steady for a while, the exponential in Eq 5 has taken the complementary function to zero, and the instantaneous displacement is given by Eq 7 alone. Its amplitude is found using the trig relation $A \cos \omega t + B \sin \omega t = \sqrt{A^2 + B^2} \cos(\omega t + \phi)$, and it so happens that $A^2 + B^2$ in the numerator equals the denominator. The amplitude is therefore

$$|\xi| \;=\; \frac{1}{\sqrt{(M\omega^2 - S)^2 + R^2 \omega^2}}. \tag{8a}$$

You may prefer this in terms of ω_0 and τ:

$$|\xi| \;=\; \frac{1}{M \sqrt{\left(\omega^2 - \omega_0^2\right)^2 \;+\; 4 \left(\frac{\omega}{\tau}\right)^2}}. \tag{8b}$$

The phase of the displacement satisfies

$$\tan \phi \;=\; \frac{2\omega/\tau}{\omega^2 - \omega_0^2}.$$

A graph for the case $M = S = 1$, $R = 1/10$ is plotted in Figure 20. Top of the peak, where $d\xi/d\omega = 0$, is at

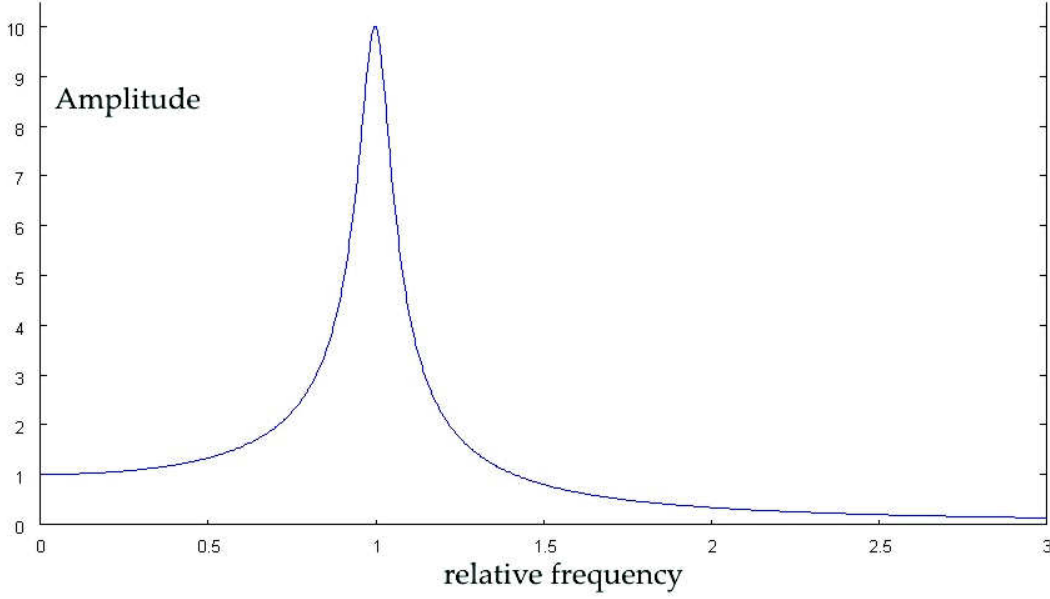$$\omega_{pk} \;=\; \sqrt{\frac{S}{M} - \frac{R^2}{2M^2}} \;=\; \sqrt{\omega_0^2 - \frac{2}{\tau^2}} \tag{9}$$

23

Figure 20: Theoretical frequency response of a damped harmonic oscillator driven at frequency ω, plotted as function of ω/ω_0. Case $M = S = 1$, $R = 1/10$.

which, interestingly, is not the same as the damped resonance frequency of Eq 5. In the example of Figure 20 it is all of $99 \cdot 75\%$ of the undamped resonance. The value at the maximum is $1/(R\omega_d)$. The velocity of the vibrating mass is obtained by differentiating Eq 7:

$$\dot{\xi} \;=\; \frac{1}{H}(R\omega^2\cos\omega t \;+\; \omega(M\omega^2 - S)\sin\omega t) \tag{10}$$

where H is the denominator of Eq 7. Now it is common in vibration studies to consider the applied force as a complex quantity $e^{i\omega t}$ and define a complex mechanical impedance as the applied force required to produce unit particle velocity. The impedance Z can be shown to be

$$Z \;=\; R + i\left(M\omega - \frac{S}{\omega}\right). \tag{11}$$

The real part is the resistance causing energy dissipation, and the imaginary part is the reactance. It is usual to define the resonance to be where the reactance is zero, which is where $\omega^2 = S/M = \omega_0^2$. You will see from Eq 10 that this is where the velocity component which is out of phase with the $\cos\omega t$ driving force is zero. Though ω_0 is different from the peak ω_{pk} in Eq 9, for low damping the difference is barely detectable.

The broadening of the peak in more significant – note the strong similarity to the frequency response of the wine bottle in Figure 9a, including the raised shoulder on the low frequency side. The Q factor for a resonance is the reciprocal of the ratio (power lost : power stored) per cycle. An equivalent definition used by Morse and Ingard has Q as the number of cycles which elapse, at ω_0, for the amplitude to reduce to $e^{-\pi} = 4 \cdot 3\%$ of its initial value once the driving force is switched off. This is

$$Q \;=\; \frac{\omega_0 M}{R} \;=\; \frac{\omega_0 \tau}{2}. \tag{12}$$

For Figure 20 $Q = 10$, and this happens to be about Q for the Box C Helmholtz resonator whose decay curves are shown in Figures 18 and 19 [9]. For small R I calculate that the FWHH of the peak

---

[9] $\pi \times 134$ Hz $\times 0 \cdot 025$ sec $= 10 \cdot 5$

is about

$$\text{FWHH in radians/sec} = \sqrt{3}\,\frac{R}{M} = \frac{2\sqrt{3}}{\tau}, \tag{13}$$

giving about $0\cdot173$ for Figure 20. Then

$$Q \approx \frac{\sqrt{3}\,f_0}{\text{FWHH}} \tag{14}$$

where the peak frequency f_0 and FWHH are measured in Hz. This affords a method for measuring the dissipative force R in a Helmholtz resonator since we know the mass of the air plug. For the wine bottle example, the volume of the oscillating air plug is about 27 cc and the density of air at room temperature is $1\cdot22$ kg/m^3, making the mass about 33 mg. The rate of working of the dissipative force will give an upper limit (because of other loss mechanisms) for the power radiated from the resonator as sound. Interesting as this is, I will not pursue it further. I merely refer again to the wine bottle resonance in Figure 9a as an example. The FWHH is 6 Hz = $37\cdot7$ radian/sec so $\tau = 0\cdot092$ seconds. The peak is at 112 Hz so $Q \approx 112\sqrt{3}/6 = 32$. So in 32 cycles at 112 Hz, lasting about $0\cdot29$ seconds, the sound from the wine bottle will die to 4% of its initial amplitude – and become inaudible.

A final general observation: as $\omega \to 0$ the amplitude in Eq 8 a, b tends to $1/S$. As $\omega \to \infty$ it tends to $1/(M\omega^2)$. Morse and Ingard (p 48) point out that all damped harmonic oscillators are stiffness controlled at frequencies much lower than ω_0, resistance controlled near ω_0, and mass controlled well above ω_0. This is why the curve in Figure 20 is not symmetric.

Most of the above discussion applies generally to any driven damped harmonic oscillator. Theoretical estimates of the resistance R and of Q of a Helmholtz resonator are noted in §5.4. below.

5.3   Neck length correction and multiple apertures

Another caveat in relating Eq 4 to reality is that the volume of the oscillating air plug is not adequately defined by the nominal dimensions of the neck. Intuitively we know that the plug fades at one end into the ambient atmosphere and at the other end into the air in the cavity. This is accounted for by a 'neck length correction'.

Here is a simple intuitive model of the total air volume in motion at the neck, and hence the effective length of the neck. We consider an elliptical slot, length d, width w. Figure 21 illustrates three volumes of air: the plug within the neck (green), and two hemi-ellipsoidal caps (blue and turquoise), one outside and one inside the resonator cavity. Viscosity will maintain a boundary layer round the edge of the hole, making the displacement there almost zero. The maximum distance to which the ellipsoid of vibrating air extends into the ambient space is open to judgement, but it seems plausible that we will not be far wrong if we take it to be the geometric mean of the major and minor dimensions of the aperture, that is $\sqrt{dw}$. The volume of the combined external and internal caps is then $\pi dw\sqrt{dw}/6$. The sectional area of the neck is $\pi dw/4$ so the volume in the caps is equivalent to an extra length of $2\sqrt{dw}/3$ on the geometrical length L. Therefore the overall acoustic length is about

$$L_{eff} \approx L + \tfrac{2}{3}\sqrt{dw} \tag{15}$$

where d is the longer dimension of the aperture, w the shorter. This includes a cylindrical neck of diameter d as a special case: $L_{eff} \approx L + 2d/3$. In a violin the top plate is only about 3 mm thick compared with the long dimension of an f-hole of about 75 mm. The neck correction therefore will account for almost the total length of the air plug.
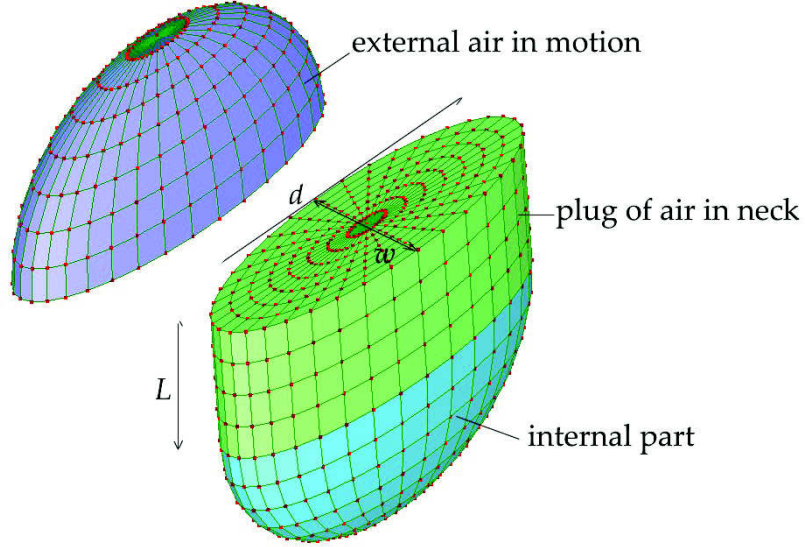
Figure 21: Simple approach to estimating the neck length correction. The shapes represent three volumes of air in vibration at the neck in the cavity. The external cap has been displaced to show the cross section.

Eq 4 was quoted without derivation in my first article in which I describe constructing the large asymmetric viola mentioned in Table 2. In that early article I reported an experiment with a glass wine bottle with parallel neck. This is a good approximation to an ideal Helmholtz resonator in that the walls are essentially rigid and there is a well-defined neck. The mechanism for exciting resonance by blowing involves eddies separating at the leading edge of the opening ('vortex shedding'), so causing pressure oscillations within the bottle. Their frequency depends on the curvature of the lip of the bottle and is proportional to the air flow rate. So, by carefully judging how hard to blow, one can match the vortex shedding frequency to the Helmholtz frequency and excite a musical note.

For my experiment then, the bottle had a nominal capacity of $0 \cdot 75$ L, with neck inner diameter $1 \cdot 88$ cm and length about $7 \cdot 5$ cm – rather ill-defined because of the curved shoulder on the bottle. Eq 4 predicts $f_{Helm} = 121$ Hz (B$\natural$), compared with B$\flat$ as heard. I found the effective value of A/L by adding water to the bottle to change the air volume. The relationship between frequency and volume (to the bottom of the neck) was close to $f^2 V = 9 \cdot 7$ SI units, making $A/L = 0 \cdot 00325$, compared with $0 \cdot 00370$ from nominal dimensions. Therefore the effective length is $8 \cdot 5$ cm, 1 cm longer than assumed. This, then, is the experimental neck length correction. Eq 15 would add $2 \times 1 \cdot 88/3 = 1 \cdot 25$ cm to the length.

A formula equivalent to Eq 4 can in principle be derived for the case of several apertures, each with its own neck. Here is my own argument for the case of two apertures. Let them have sectional areas A_1, A_2, acoustic neck lengths (following Eq 15) of L_1, L_2, and let the plugs of air contained within have masses m_1, m_2 and undergo displacements x_1, x_2 as the pressure within the resonator increases by δp. The forces moving the two plugs of air are respectively $A_1 \delta p$ and $A_2 \delta p$ so the equations of motion are

$$\frac{A_1 K}{V} \delta V \;=\; -m_1 \frac{d^2 x_1}{dt^2}, \qquad \frac{A_2 K}{V} \delta V \;=\; -m_2 \frac{d^2 x_2}{dt^2} \, .$$

Again K is the bulk modulus and δV, the change in volume, is $A_1 x_1 + A_2 x_2$. As in §5.1 we look

for periodic solutions where $x_1 = b \cos \omega t$ and $x_2 = \cos \omega t$, b being the ratio of the amplitudes. The coupled equations of motion are

$$A_1 K (A_1 b + A_2) + b m_1 V \omega^2 \; = \; 0, \qquad A_2 K (A_1 b + A_2) + m_2 V \omega^2 \; = \; 0 \tag{16}$$

and their solution is

$$\omega^2 \; = \; \frac{K(A_2^2 \, m_1 + A_1^2 \, m_2)}{m_1 m_2 V}, \qquad b \; = \; \frac{A_1^2 \, m_2}{A_2^2 \, m_1}. \tag{17}$$

Using $M_1 = A_1 L_1 \rho$, $M_2 = A_2 L_2 \rho$, $K = c^2 \rho$ we arrive at

$$\omega \; = \; \frac{c}{2\pi} \sqrt{\frac{1}{V} \left[\frac{A_1}{L_1} + \frac{A_2}{L_2} \right]}, \qquad b \; = \; \frac{L_2}{L_1} \tag{18}$$

The formula admits to only one resonance since there is only one 'spring', despite there being two holes. It also implies that the aperture with the largest ratio of area to effective neck length will dominate. This is plausible – a wide hole in a thin shell offers a smaller impedance to motion than a long narrow neck.

5.4   Other theory of the Helmholtz resonance

Many experimental and theoretical studies have been made of air resonators, but I don't intend to give a lengthy review. Analysis to quantify the effective length L_{eff} was first developed by Helmholtz and Lord Rayleigh and reported in volume II of the latter's monumental 'Theory of Sound'. Rayleigh's detailed Chapter 16 approaches the problem in three ways, considering in turn the aperture as a hole in an infinitesimally thin wall, then in a wall of finite thickness, then as the open end of a cylindrical pipe. Using first an electrical analogy with the capacitance of an insulating plate with aperture in a conducting matrix, Rayleigh gives this formula for the resonant frequency

$$f \; = \; \frac{c}{2\pi} \sqrt{\frac{\mathscr{C}}{V}}$$

where $\mathscr{C}$ is the 'conductance' of the aperture. Now the conductance of a length L of electrical wire, sectional area A, is proportional to A/L – the reciprocal of its resistance – so similarly the acoustic conductance of an aperture is A/L, giving Eq 4. Moreover, just as the total conductance of a collection of parallel electrical resistors is obtained simply by adding, so n holes have an aggregate acoustic conductance $\sum A_n/L_n$, giving us Eq 18 again.

Rayleigh discussed several ways of quantifying $\mathscr{C}$. Neglecting all damping, he analysed the case of an elliptical aperture in a thin flat plate, obtaining an exact result (within his assumptions) in terms of elliptic integrals. Ellipses of all aspect ratios had conductances greater than that of a circle *of equal area*, but the increase is only 20% for an aspect ratio as large as 6. He concluded that $\mathscr{C}$ for any oval slot will be just slightly larger than that of a circular aperture having the same area.

Rayleigh goes on to estimate that the length correction (counting both ends) for a circular aperture of diameter d lies between

$$\frac{\pi d}{4} = 0 \cdot 785 \, d \;\; \text{and} \;\; \frac{8d}{3\pi} = 0 \cdot 849 \, d, \tag{19}$$

with the most likely value being about $0 \cdot 82 \, d$. This is to be compared with the $2d/3$ proposed in §5.3. For oval holes he proposes replacing d by $2\sqrt{A/\pi}$, which gives the same area.

The theory of damping by radiation appeals to arguments which replace the aperture by a thin massless oscillating piston of air in a rigid wall. Related arguments compare the opening in the resonator's neck with the open end of a long pipe, with or without flange. A formula applying to damping by radiation only is quoted in another textbook[10]. It leads to the formula for Q

$$Q = 2\pi \sqrt{V \left(\frac{L_{eff}}{A}\right)^3} \qquad (20)$$

where L_{eff} is the effective length of the air plug at the neck. However, I don't find this formula very useful. Applied to the wine bottle with $V = 750$ cc, $L_{eff} = 9$ cm and $A = 3\cdot12$ cm^2, it gives $Q = 843$!

Morse and Ingard (Chapter 9) spend several pages developing analogies between electrical and acoustic circuits. They develop expressions for my M, R and S of §5.2 above, where the resistance R allows for both radiation and viscous damping. They take into account the phase changes by calculating the complex impedance of the piston, resistance plus reactance. The reactance relates to the piston pushing sound back into the cavity where a standing wave builds up. For a circular piston their results for viscous damping only[11] are (page 490)

$$\omega_0 = c\sqrt{\frac{4A}{DV}}, \qquad Q = \sqrt{\frac{2D}{b\ln\frac{16A}{\pi h^2}}}. \qquad (21)$$

where D is the perimeter of the opening, A its area and h the thickness of the plate, assumed thin. b is the thickness of the boundary layer: $b = \sqrt{2\mu/(\rho\omega)}$ for air vibrating at f Hz. Using μ, the dynamic viscosity at 18 μPa sec and ρ, the density at 1.25 kg/m^3, b is about $0\cdot00214\sqrt{f}$ metres. Morse and Ingard therefore predict that Q should vary as $f^{1/4}$ because of viscosity. For a circular aperture their formula for the resonant frequency ω_0 has $D = \pi d$ so corresponds with an effective length to the plug of air in the aperture of $\pi d/4$, as previously obtained by Rayleigh, Eq 19. Their formulae are not applicable to the wine bottle because of its extended neck, but would apply to violin f-holes. Taking $f = 270$ Hz, $A = 1100$ mm^2 for both holes, $D = 4 \times 80$ mm and $h = 2\cdot4$ mm gives Q about 27, a reasonable value. In §3.1 I report for the violin in Figure 9b that FWHH is about 11% of the resonant frequency A0, corresponding to Q being about 17.

In an interesting paper[12] Michael Moloney carried out experiments on three bottles with necks, very similar to my own experiments described above and in the next section. He makes careful comparison with theory regarding both the acoustic conductivity of the neck and the Q factor. He finds for the 750 cc bottle which looks most like mine that Q is about 40 to 45 depending on frequency. This compares with the 32 I found for the empty bottle. However, the Q due to radiation alone was between 1170 and 1970, of the same magnitude as the 830 I calculated. Moloney presents a theory of viscous losses which, as expected, occur mainly in a thin boundary layer around the inside of the neck. There, on the glass side, the air is stationary, but moving at full speed a fraction of a millimetre away. Like Morse and Ingard, he finds an increase in Q with frequency, and shows that Q due to viscous losses at the inner bottle wall is in the range 43 to 56. Therefore Q is dominated by viscous losses and radiation makes but a small contribution. I find some support for the $f^{1/4}$ dependence of Q in Molloney's experimental results. Fitting a power-law trend-line to his

---

[10]The Science and Application of Acoustics by Daniel Raichel, Springer, 2000. There are misprints on p145 where at equations 7.60a, b k should read k^2. Similar reasoning is used to estimate the sound radiated from the open end of a tube, with or without flange.

[11]They give a much more complicated formula which includes radiation damping.

[12]Am. J. Physics, Vol 72 p1035, 2004. I carried out my experiments before coming across Moloney's paper.

five data for the 75 cc wine bottle, I find scatter about a power law $Q \approx 10 \cdot 7^{\,0 \cdot 28}$, though for his other two bottles the exponent is about $0 \cdot 36$.

Another interesting paper is by Guy Vandergrift[13]. He had been using the air resonance of a violin as a teaching tool for students on the damped driven harmonic oscillator. He describes three ways for measuring the Q-factor of the resonance and discusses several of the approximate analytical approaches to determining its frequency, but concludes that

> 'We see that a large number of complications make it very difficult to calculate the resonant frequency to precision better than 10%.'

In my study I have circumvented many of these complications and approximations by using finite element analysis, which deals with all the geometrical complications of the shape and size of the aperture. Its main limitation is that it assumes rigid walls.

6 Helmholtz resonance of a wine bottle by experiment and FEA

The spectrum in Figure 9a shows that a wine bottle has a simple resonance. I had measured the end correction in my previous article, as summarised in §5.3. However, I decided to measure it again, on another bottle, with the aim of making a close comparison with finite element modelling using the LISA program. This was a starting point for FEA of a variety of openings, leading to modelling the f-holes of a violin (see §7.2).

6.1 Measurements on a bottle

The bottle became available after enjoying the 750 cl of Gran Familia tempranillo it contained. The method used this time was for me simply to blow across the open neck and record the sound with an external microphone about half a metre away. Water was added to the bottle in stages to reduce the volume of air, the amount being determined by weighing the bottle and contents. The Helmholtz frequency was determined as a function of cavity volume, as listed in Table 3.

Total weight (g)	Weight water (g)	Volume cavity (cc)	Meniscus height (mm)	Frequency (Hz)
476	0	740	0	115
520	44	696	20	120
638	162	578	57	130
720	244	496	78	140
798	322	419	100	152
872	396	345	120	168
949	473	268	140	194
1032	556	185	163	226
1107	631	110	181	291
1136	660	81	189	339
1178	702	39	202	454
1190	714	27	206	523
1216	740	1	223	

Table 3: Measurements of the musical note produced by blowing across a wine bottle
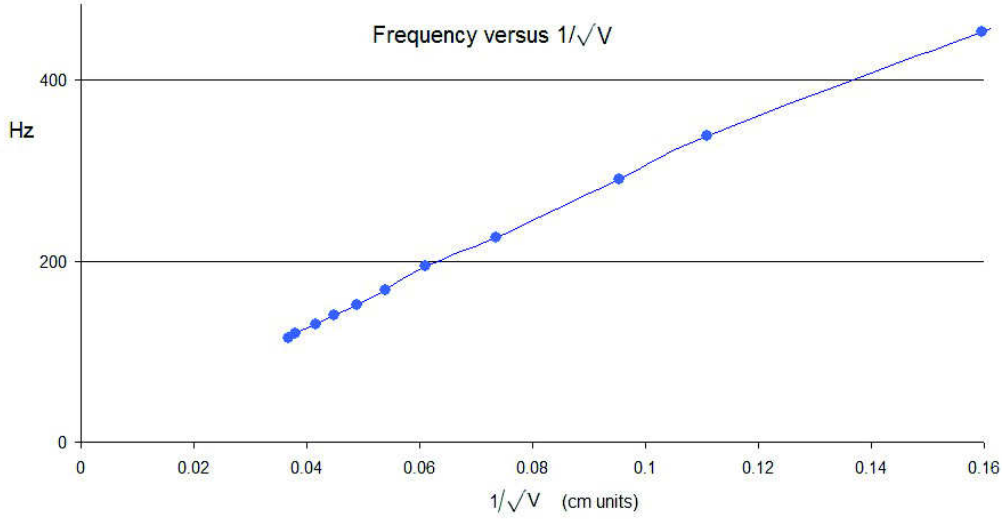
[13]Am. J. Phys. Vol 61 No 5 May 1993, p 415-421.

Figure 22: Experimental values of Helmholtz frequency and volume of air in the body of the bottle plotted as f against $\frac{1}{\sqrt{V}}$.
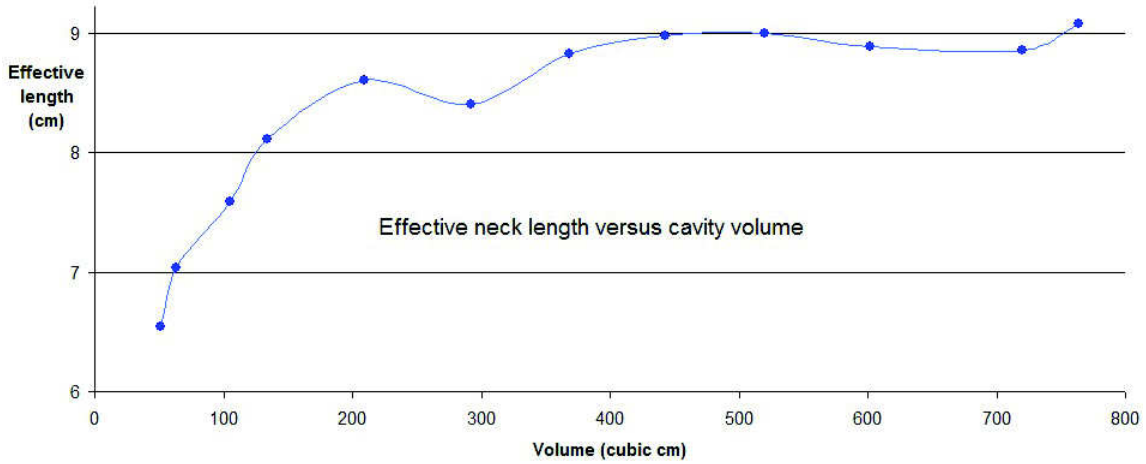

Figure 23: Effective neck length as a function of air volume in the wine bottle.

Here are some experimental details. The signal was digitised in a computer at 44,100 Hz and captured with the GoldWave software with the resonant frequency determined by spectrum analysis using the WaveSpectra program. Various spectrum window functions and running sample lengths were tried, but the results were satisfactorily consistent. The accuracy of frequency recording and spectral measurement was checked at 440 Hz by listening to beats against a mechanical tuning fork. The uncertainty in the Helmholtz frequency is less than 5 Hz. The scales were also calibrated against known weights and found to be correct and reproducible to within 2 grams. The water was cool, from the tap, and the air temperature about 16° to 17°C. The velocity of sound in air c depends on temperature $T°$C according to $c = 331 \cdot 3 + 0 \cdot 606T$ so at this temperature it was $341 \cdot 5$ m/sec.

The internal dimensions of the bottle had to be measured as accurately as the tools available would allow so that the finite element mesh model would be a close representation of reality. The water height to the water meniscus measured with a rule as a function of weight allowed the internal diameter to be determined. The neck was not an exact parallel cylinder. Its internal diameter was

determined by adding water 5 ml at a time from a calibrated clinical syringe and measuring the height to the meniscus. I fitting a cubic curve to the graph of volume against height, differentiated analytically to obtain the sectional area as a function of height, and converted to diameter. This was adjusted by about 2% to be consistent with photographs of the neck taken with a bright light behind. The diameter at a distance about 1 cm into the neck as measured with callipers was $1 \cdot 92$ cm. The total volume of the bottle was 764 cm^3 (ml or cc), with the volume of the neck being about 24 cc. Therefore its sectional area was $3 \cdot 12$ cm^2.

Classic theory, Eq 4, predicts that frequency will increase proportional to $1/\sqrt{V}$, V of course being the volume of the cavity excluding the neck. Figure 22 is a graph to test this. There is only modest departure from a straight line through the origin.

At each stage in changing the volume the effective length of the neck in Eq 4 can be found to make the predicted frequency agree with the measured. Values so obtained are plotted in Figure 23; it is typically $8 \cdot 9$ or $9 \cdot 0$ cm. The actual neck length is about $7 \cdot 7$ cm, as near as can be judged from where the internal shoulder begins. The length correction is therefore almost constant at about $1 \cdot 3$ cm until the volume of the cavity (up to the shoulder) becomes small, when it decreases rapidly, even becoming less than the physical length, *i.e.* the 'spring' extends a little into the neck.

In a final set of tests I produced the bottle's note with a hair drier instead of blowing. The drier had four temperature settings, allowing a rough assessment of the effect of velocity of sound on the resonance. The air temperature measured about 10 cm from the drier was 16°, 22°, 31° and 46°C respectively on the four settings. With the drier on cool, the bottle's note was the same as when blowing by mouth. With the bottle empty the frequency increased from 171 to 178 Hz between the cool and hottest settings. With the water level up to 177 mm it increased from 275 to 289 Hz. This 5% increase corresponds almost exactly with the ratio of sound velocities at 46° and 16°C – $358 \cdot 3 / 341 \cdot 1$. A further increase to 299 Hz was achieved by first blowing the hottest air stream directly into the bottle and allowing it to warm up for a couple of minutes. This is a 9% increase, well over a semitone.

6.2   Finite element modelling of the bottle

The author was privileged to have an evaluation, pre-release copy of the LISA 8 finite element program. One of its analysis types is solution of the Helmholtz equation for standing acoustic waves in an air space bounded by rigid walls. The total pressure in the gas is a constant ambient p_0 modulated by a small sinusoidal acoustic addition $p_a(x, y, z) \cos \omega t$ at position (x, y, z). The wave equation then implies Helmholtz's time independent equation for p_a

$$\nabla^2 p_a \;=\; \frac{1}{c^2} \frac{\partial^2 p_a}{\partial t^2} \quad \text{implies} \quad \nabla^2 p_a + \frac{\omega^2}{c^2} p_a = 0$$

where c is the velocity of sound. Though LISA's method is restricted to totally closed spaces with rigid boundaries, it is possible to model a rigid object with apertures such as an open bottle if it is embedded in a much larger outer space, a 'room', which itself is closed. One solves for many normal modes, most of which relate to standing waves in the room. However, it is possible to distinguish resonances of the bottle alone because then the air in the room is all at the same uniform pressure.

The mesh is shown in Figure 24. This models the air in the bottle, the glass being its boundary. Glass is essentially rigid, as is assumed in solving Helmholtz's equation. Note the slight taper of the neck. For Helmholtz's equation LISA 8 allows only linear hex8 elements, so that it what
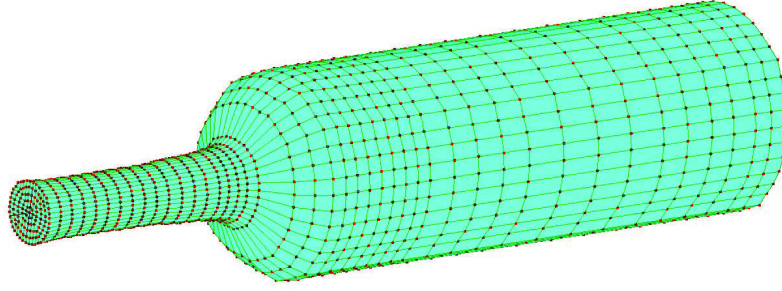
Figure 24: The wine bottle modelled as a finite element mesh.

the mesh is built from. There are 1,600 elements in the neck, 2,700 in the rest of the bottle. The outer room was roughly cylindrical, 150 cm diameter and 200 cm long, though in the analysis these dimensions were varied to ensure that air cavity modes were correctly identified. There were 17,920 elements in all, and 21,057 nodes. The solution calculates the pressure amplitude $p_a(x, y, z)$ at each node, meaning that the standing wave is $p_a(x, y, z) \cos(2\pi f_n t)$, where n is the mode number. Figure 25 shows a longitudinal section through the 3D model at the Helmholtz resonance, f_0. Observe that all the change in pressure occurs within the neck; the pressures in the external space and inside the bottle are constant, at opposite extremes of those predicted.

The bottom (right hand in the picture) part of the bottle was moved and/or deleted in steps to simulate a rising water level. LISA has the facility to measure the volume of selected elements and this was used to set the model volume to be within $0 \cdot 5$ cc of each of the volume values used in the experiment to allow a point by point comparison. Some early trials showed that the predicted frequencies were quite sensitive to the precise dimensions of the air space, which accordingly were checked again. Taking the velocity of sound to be 34,100 cm/sec the predicted Helmholtz frequencies are as listed in Table 4, compared with the experimental values. I consider this agreement to be good, considering the limited tools for measuring the internal dimensions of the bottle and the slight uncertainty in the air temperature in the neck.
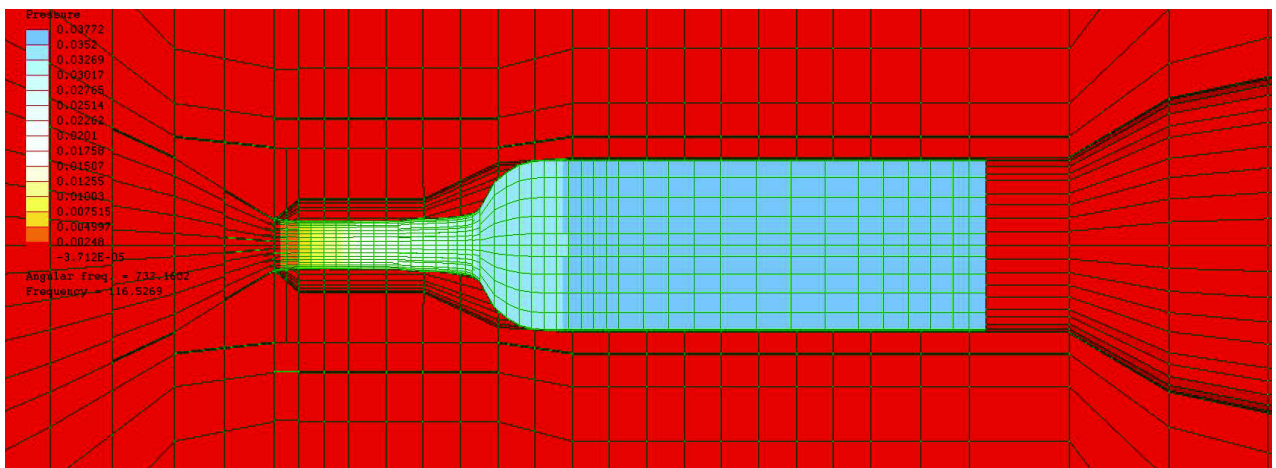

Figure 25: Section through the FE mesh at the Helmholtz resonance of $116 \cdot 5$ Hz, showing pressure contours.

Total air volume (cc)	Expt Freq Hz	LISA 8 Hz	Diff Hz	% diff
764	115	116·5	1·5	1·3
720	120	120·3	0·3	0·2
602	130	132·5	2·5	1·9
520	140	143·4	3·4	2·4
443	152	156·4	4·4	2·9
369	168	172·5	4·5	2·7
292	194	196·1	2·1	1·1
209	226	235·4	9·4	4·2
134	291	301·8	10·8	3·7
105	339	348·2	9·2	2·7
63	454	473·0	19·0	4·2
51	523	550·8	27·8	5·3

Table 4: Comparison of Helmholtz frequency predicted by LISA FEA with experimental values for a wine bottle at 16°C.

It is instructive to relate the pressure contours predicted by finite element modelling to the air plug and spring model of the classic Helmholtz theory, Figure 17. Figure 26 plots the amplitude of the acoustic pressure p_a along the axis z of the empty wine bottle from the LISA solution; the units are arbitrary. Recall that the total pressure at position (x, y, z) is $P_0 + p = P_0 + p_a(x, y, z) \cos \omega t$. $p(0, 0, z, t)$ is zero outside and well away from the bottle, increases linearly with position through the neck, and attains an almost constant, largest value at the bottom of the bottle. The wavelength far exceeds the length of the bottle so all particles move in phase. The variation in p_a at small distances x, y off axis is small zero so the values in Figure 25 are essentially for a one-dimensional situation.

Consider a small element of gas on the z axis between z and $z + \delta z$ and with sectional area A. The instantaneous pressure difference across its faces is $p(z + \delta z) - p(z) \approx \partial p / \partial z . \delta z$. This produces a net force causing acceleration towards the lower pressure region:

$$\frac{\partial p}{\partial z} \delta z \, A \;=\; -\rho A \delta z \, \frac{\partial^2 \xi}{\partial t^2}$$

where ξ is the displacement of the element. Therefore acoustic pressure and displacement are related by

$$\frac{\partial p}{\partial z} \;=\; -\rho \frac{\partial^2 \xi}{\partial t^2}. \tag{22}$$

Noting that the peak amplitude p_a is not a function of time, ξ is obtained by integrating the acceleration twice with respect to t

$$\text{particle velocity} \;=\; \frac{\partial \xi}{\partial t} \;=\; -\frac{1}{\rho \omega} \frac{\partial p_a}{\partial z} \sin \omega t.$$

$$\text{displacement,} \; \xi \;=\; \frac{1}{\rho \omega^2} \frac{\partial p_a}{\partial z} \cos \omega t. \tag{23}$$

The displacement is therefore in phase with the pressure and proportional to the pressure gradient. Figure 27 plots the peak particle displacement along the z axis obtained by numerical differentiation of p_a from Figure 26. The plug on air in the neck is very apparent. Though it does not have sharp edges, most of it lies within 10 cm, consistent with the $9 \cdot 0$ mm obtained experimentally.
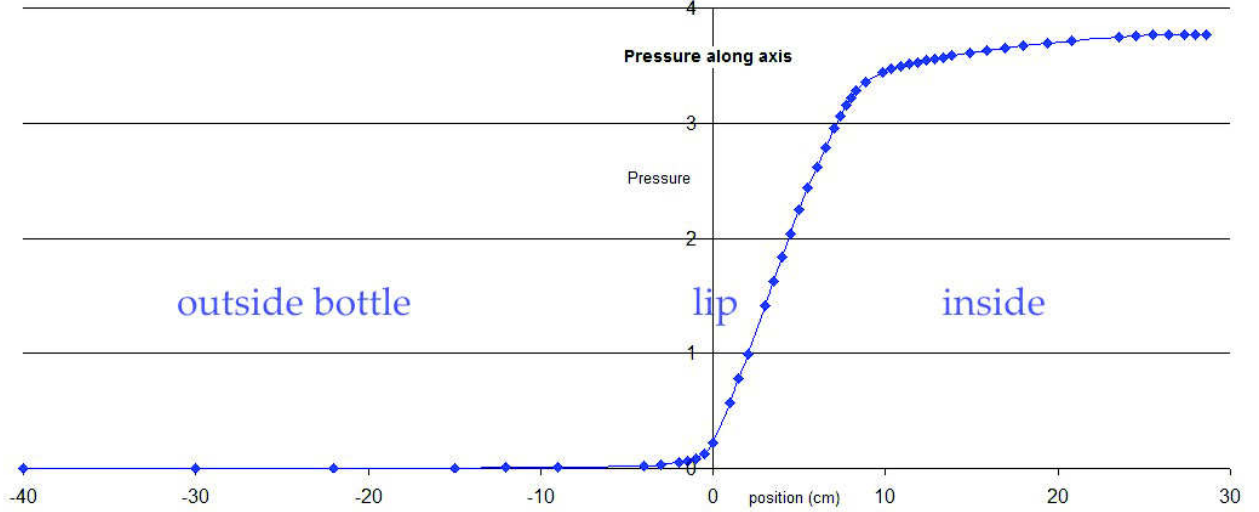
Figure 26: Finite element results for peak acoustic pressure $p_a(z)$ along axis z of empty wine bottle.
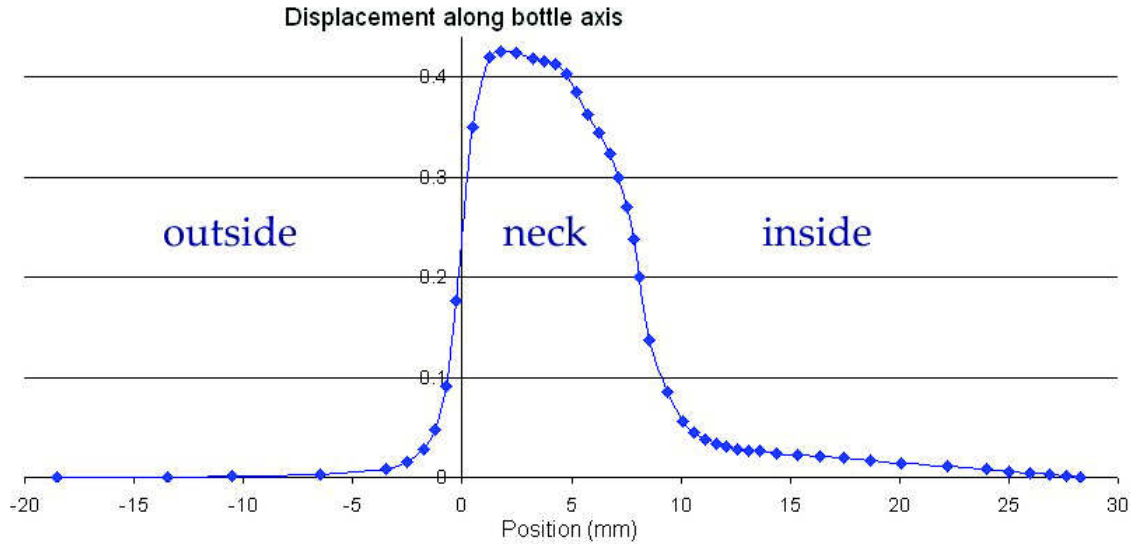

Figure 27: The particle displacement (arbitrary units) along axis z of empty wine bottle showing that almost all movement occurs in the neck.

7 Helmholtz resonances of wooden box structures

This section moves towards understanding the Helmholtz resonances of a violin using experimental measurements and finite element modelling with LISA 8. First a rectangular plywood box with flat sides is studied as a series of holes of increasing size and complexity are cut into its top plate. Call this Box A ; it was the first stage in creating the Box C used in §2. I soon discovered that the flexibility of the flimsy structure has a very significant effect in decreasing the Helmholtz frequency. Next the air cavity of a violin in modelled in finite elements and compared with the frequencies determined in §3.

Figure 28: Plywood Box A with 9 and 11 mm holes, and cable for internal electret microphone.

7.1 Rectangular plywood box with various apertures

Figure 28 is a photograph of Box A when only two small holes have been cut into it. Most measurements of the Helmholtz frequency were made in the arrangement of Figure 6 with an internal electret microphone and applied vibration from a loud speaker directed at the aperture and driven by a sine wave source. However, a few were made with the arrangement of Figure 2, with the electromechanical vibrator and external audio microphone. I started with a single circular hole, labelled α, and gradually increased its diameter and added a second hole β. Later these were merged into a slot as shown in Figure 29. The various stages and their measured Helmholtz frequencies are listed in Table 5.

In Table 5 the notation in columns 2 and 3 is as follows. First a single hole $9 \cdot 2$ mm diameter was cut (Case 1), then enlarged to 11 mm (Case 2), then a second hole, $8 \cdot 2$ mm was cut (Case 3),
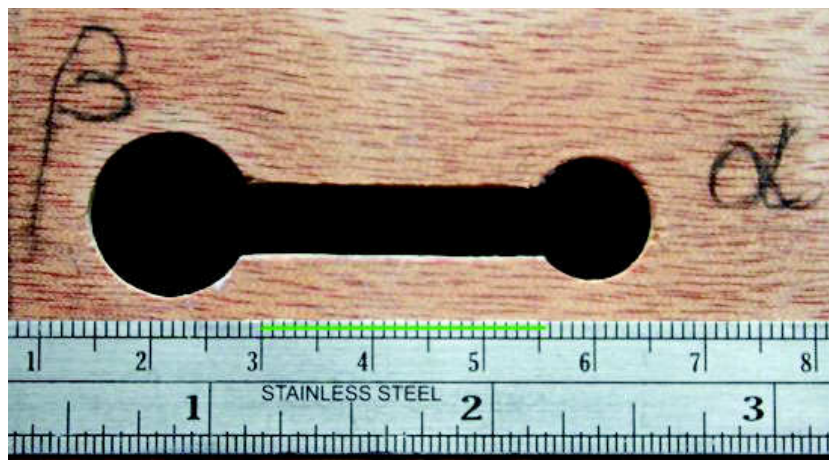

Figure 29: Detail of Case 19, a slot with circular ends cut into the top of the plywood box.

Case number	Hole diams. mm	Tube length mm	Slot width mm	Expt internal Hz	Expt external Hz	LISA FEA Hz	Classic formula Hz
Box A		3-ply box					
1	9·2, -			63		94	94
2	11, -			71		105	106
3	11, 8·2			89	123		139
4	11, 11·2			97			151
5	11, 11·2	0, 4·5		89			137
6	11, 11·2	13, 0		86			128
7	11, 14·3			103	124	153	164
8	11, 14·3	0, 11·6		91		135	139
9	11, 14·3	0, 19		88		129	132
10	-, 14·3	-, 19		57		81	82
11	-, 14·3	-, 38·7		46		64	64
12	11, 14·3	0, 38·7		82	118	120	122
13	11, 14·3	13·2, 38·7		67	97	99	93
14	11, 14·3	13·2, 0		94	102		143
15	11, -	13·2, -		52		76	75
16	11, 14·3	single slot	4·7	113	129		196
17	11, 14·3		7·3	116	121	175	195
Box B		MDF 6 sides					
18	11, 14·3	single slot	7·3	166		175	195
19	14·7, 15		14·2	180		191	201
Box C		MDF 5 sides 3-ply back					
20	14·7, 15		14·2	156		191	201
21	14·7, 15	12·5 mm clay neck	14·2	134		156	160
22	25·7, 25·7		27·9	180	185	220	240
23	25·7, 25·7	25 mm cloth	27·9	153			182

Table 5: Measured and theoretical determination of Helmholtz frequency A0 for a plywood box with various apertures and their necks.

subsequently enlarged to 11·2 mm (Case 4). Bear in mind that though a Helmholtz resonance can be detected with these small holes, its amplitude is insignificant compared with other, higher frequency resonances. For Case 5 a stub of rigid plastic tubing 4·5 mm long was affixed onto the second hole to form a neck standing proud of the plywood top. For Case 6 this stub was removed and a 13 mm long tube fixed at the first hole. A - sign means that either the respective hole had not yet been cut (Cases 1 and 2) or that it was covered up with a wooden block (Cases 10, 11, 15). At Case 16 the two holes were connected by a slot 4·7 mm wide, and this widened to 7·3 mm for Case 17.

A complete set of measurements with the internal microphone is listed under the heading 'Expt internal'. A few measurements with the Figure 2 arrangement are listed in the next column under 'Expt external'. For reasons I cannot readily explain they are all higher than with the internal microphone determination; perhaps I will return to this one day, but for now let it pass. The penultimate column is the LISA FEA model values assuming rigid cavity walls. The final column is the result of the simple formulae Eq 4 and 15 or 18 and 15. Generally they agree well with the FEA predictions.
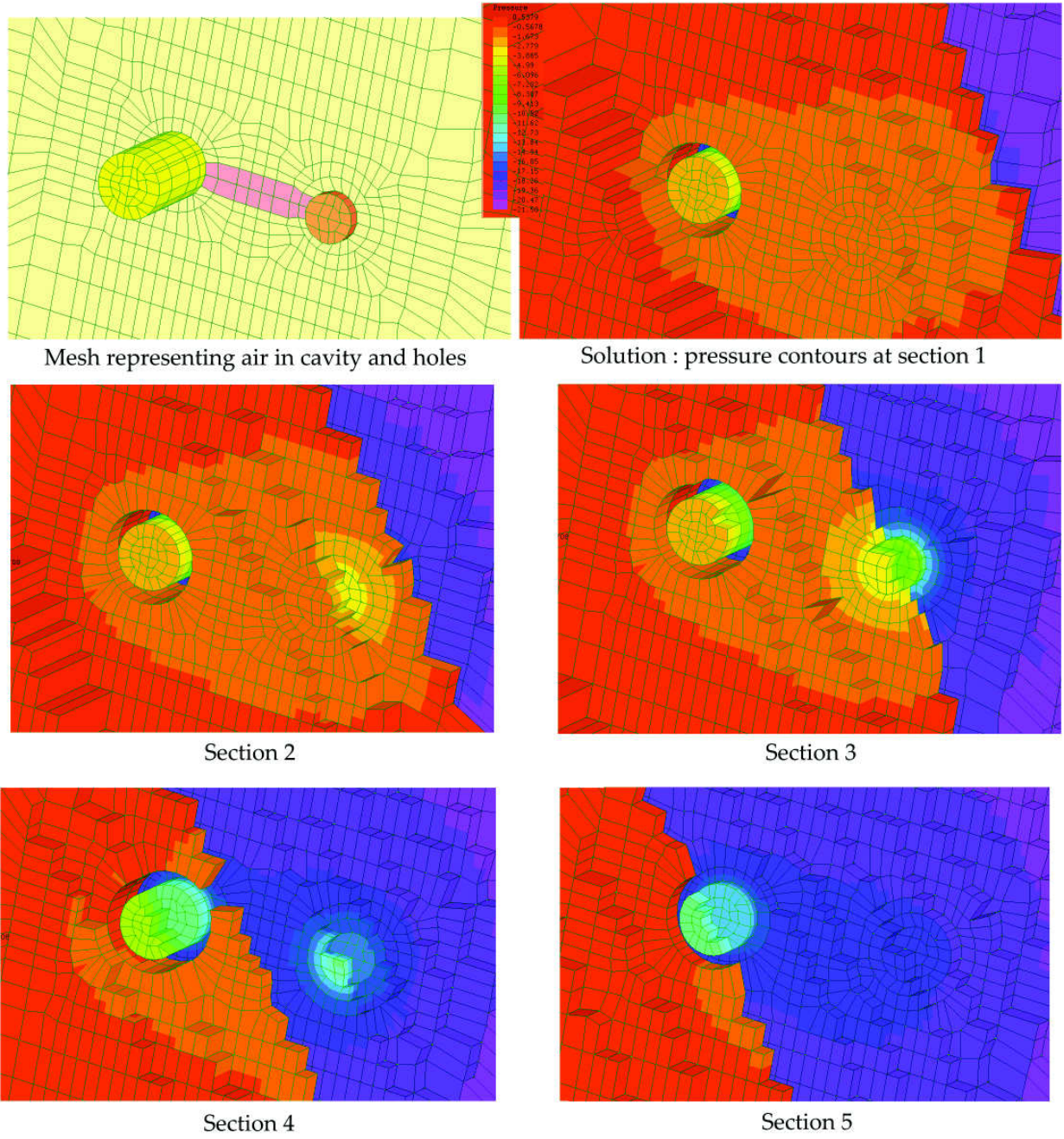
Figure 30: FE modelling of the two holes, one with 19 mm tube attached, joined by a slot. Top left: the FE mesh component representing the air in the aperture and inside the box. Others: contours of acoustic pressure at five adjacent sections through the solution space.

Figure 30 illustrates the finite element analysis applied to Case 9 in Table 5. The top left panel shows a detail of the mesh itself. Bear in mind that the elements represent air. The external air is suppressed (not visible) in this picture so that we can see the 19 mm column of air in the tube (bright yellow) and the shorter stub of air in the other hole (orange) which is only through the thickness of the plywood. The purple area between is where the slot will subsequently be formed, but at this stage it is not raised above the air inside the box (cream). The other five panels show the

solution. Colours define contours of acoustic pressure according to the scale shown. The five panels are adjacent sections through the solution space, and can be compared with Figure 25 for the wine bottle.

It was abundantly clear that the experimental values were only about 65% of the theoretical ones. I suspected that this was due to the flexibility of the box's walls increasing the overall compliance – a softer spring in Figure 17 – so reducing the natural frequency. To test this I glued some plates of $12 \cdot 5$ and 19 mm thick MDF board to all six faces of the box, leaving a hole around but clear of the slotted aperture. Call this Box B. At Case 18 we see that A0 has jumped from 116 Hz to 167 Hz, satisfactorily close to the FEA prediction of 175 Hz. Five other cases were constructed:

- Case 19: slot widened to $14 \cdot 2$ mm, shown in the photograph of Figure 29.

- Case 20: the MDF and back plate were removed from the box and a new thin pink 3-ply back plate glued on to form Box C as first described in §2. The internal microphone found A0 at 156 Hz, showing how a modest increase in flexibility will reduce A0, down from 167 Hz.

- Case 21: as Case 20, except that the thickness of the slot was increased by moulding modelling clay around it to form a neck $12 \cdot 5$ mm thicker (thickness of the MDF). A0 fell to 134 Hz.

- Case 22: the Plasticine was removed and the aperture increased to 61 by 28 mm as shown in Figure 1.

- Case 23: I glued a skirt of Dralon fabric around the perimeter of the hole to form a soft neck nominally 25 mm long.
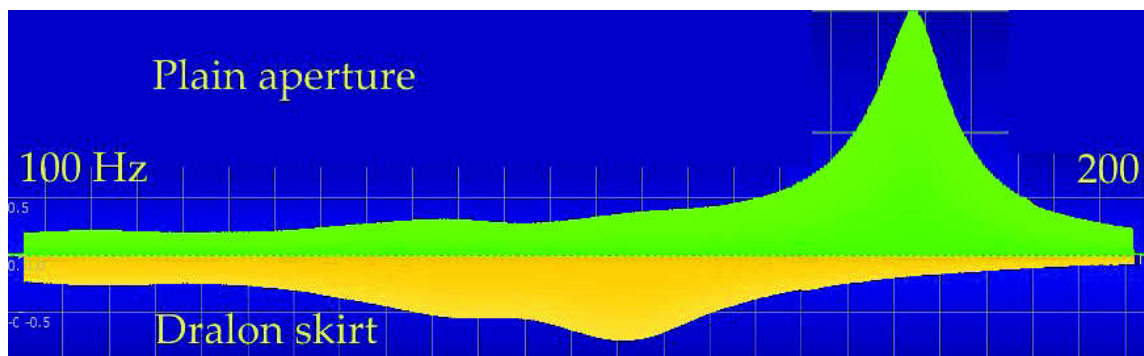

Figure 31: Effect of adding a neck (or skirt) of Dralon cloth (orange inverted spectrum) all around the perimeter of the 61 by 28 mm aperture in Box C. Upper green curve is for the aperture with no Dralon. 100 to 200 Hz.

With Case 23 I was interested to see if this velvety cloth would dampen the resonance and increase Q so that pitches over a wider interval would be evenly enhanced by the resonance. This was on the premise that, for good violin tone, one needs reinforcement of the sound whist avoiding narrow intervals of pitch in which the sound is excessively magnified. The effect of the Dralon can be seen in Figure 31. Much as with a rigid material, the cloth does form an effective neck capable of flattening A0. The peak for the plain aperture is reduced to about 40% of its amplitude (16% of its power) but so is the amplitude at 200 Hz. The FWHH of the unadorned plain aperture is from 175 to $184 \cdot 5$ Hz, centred at 180 Hz. Hence from Eq 14 Q is 33. For the Dralon-dressed aperture FWHH is from 130 to 167 Hz, centred on 153 Hz, so Q is only 7. A large aperture with cloth neck could be fashioned to have the same A0 frequency as a conventional violin f-hole, and on this evidence would enhance the tone over a wider pitch interval. An interesting conjecture.

7.2   FE model of violin air cavity

To round off this study using finite element models I have constructed a fair approximation to the air cavity and f-holes of a violin in LISA. Figure 32 is a detail of one f-hole, showing that it is 74 mm end to end and $6 \cdot 2$ mm wide near its centre. The circular end hole nearer the upper bout is $5 \cdot 5$ mm diameter and the larger towards the lower bout is $9 \cdot 3$. The wood here is $2 \cdot 4$ mm thick. By plotting an enlarged profile of the hole in LISA I find the area of the hole to be 550 mm^2.
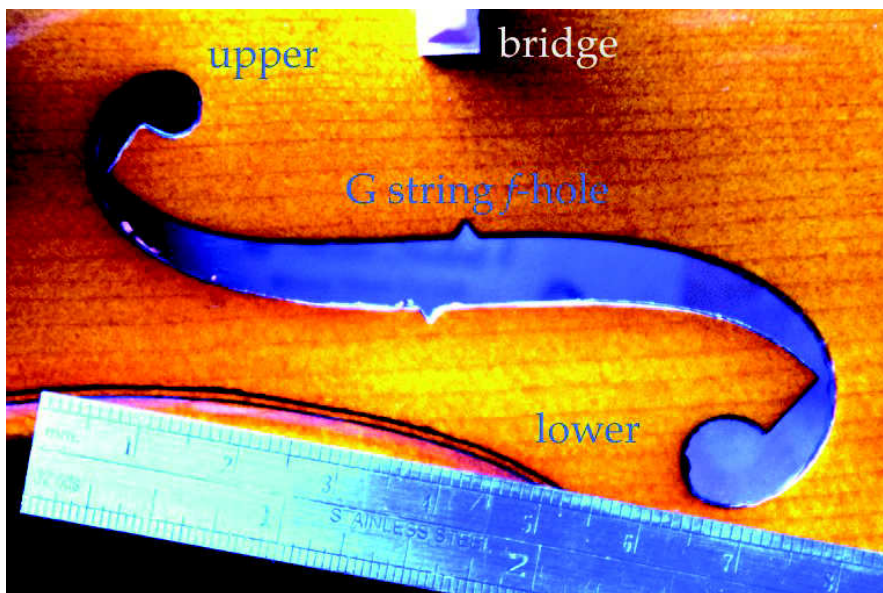

Figure 32: Detail of the f-hole next to the G string of a factory-made violin.
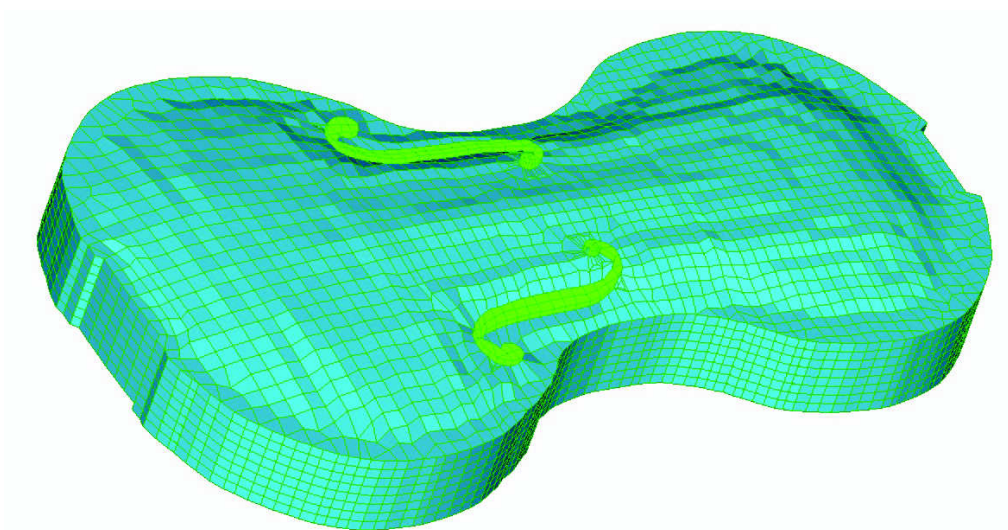

Figure 33: Mesh model of air cavity within a violin, with f-holes.

The air cavity and f-holes were modelled closely as an entirely hex8 mesh in LISA 8, including making an approximation to the domed plates. Figure 33 shows the finite element mesh of the air space, with cut-outs where the six internal supporting blocks are placed. The external 'room' of air encompassing the violin is here rendered invisible to reveal the embedded violin. The volume of the air cavity, excluding the holes, is $0 \cdot 002073$ m^3, about 2 litres, as determined from the mesh. The A0

39

frequency predicted on the assumption that the walls are rigid is 312 ± 2 Hz, to be compared with the experimental 267 Hz reported in §3.1. Assuming that LISA predicts correctly the frequency for a rigid cavity, the effect of elastic wood compliance is to reduce A0 to about 86% of its rigid-wall value. This is not inconsistent with the reduction to 65% for the more flexible plywood Box A of §7.1. Figure 34 is a section through the solution mesh at the position of the f-holes showing contours of acoustic pressure. Notice that the internal pressure is not constant as the simple theory assumes, but varies by about 50% between the upper and lower bouts.

Figure 35 is a similar plot at A1 in which a half wave-length fits lengthwise into the cavity. The predicted frequency is 512 Hz, compared with 474 measured – some 93% of the predicted. The pressures in the two bouts have opposite phase.
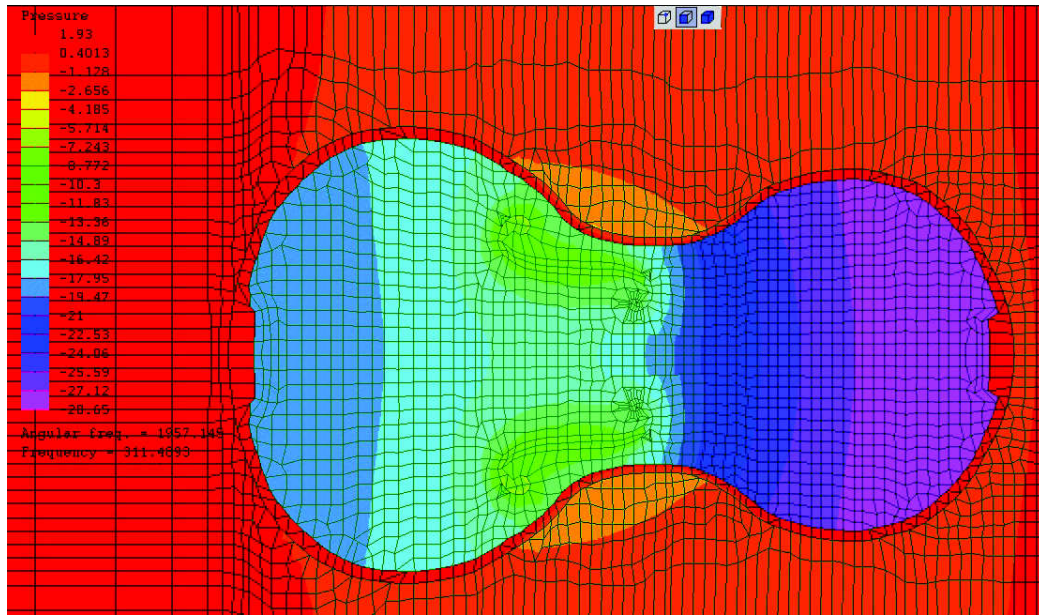

Figure 34: Contours of sound pressure at the A0 Helmholtz resonance at 312 Hz as predicted by LISA. Section through the f-holes.
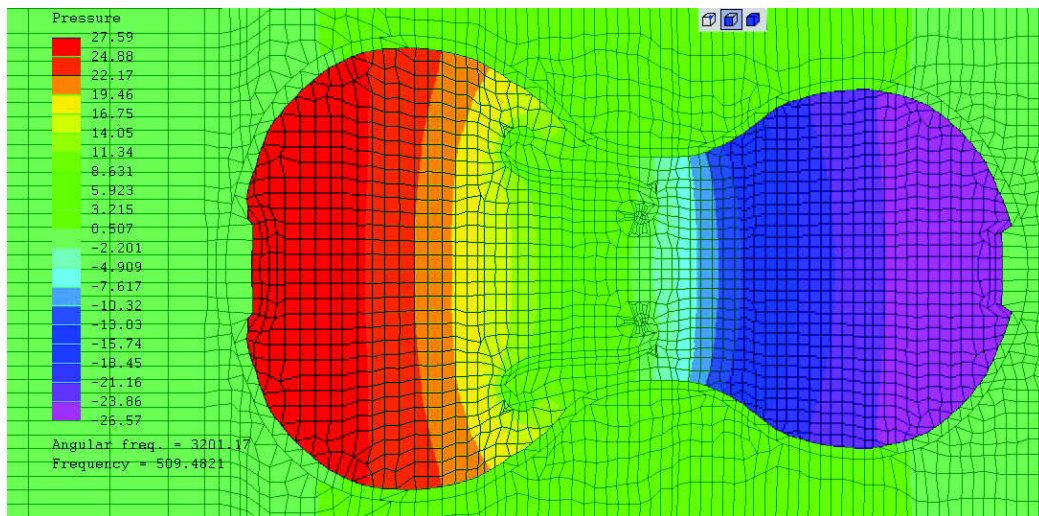

Figure 35: Contours of sound pressure at the A1 resonance at 511 Hz.

8 Effect of wood flexibility on Helmholtz frequency

Table 5 shows clearly the large reduction in the Helmholtz A0 frequency when the cavity walls are flexible instead of rigid. This means that finite element solutions of Helmholtz's equation using LISA will give an upper bound to A0 for a violin or viola, the precise over estimate depending on the flexibility of the violin. This section considers models which aim to quantify the effect.

8.1 Simple mass and spring model

I start with a simple model of my own devising which essentially treats the flexibility of the cavity walls as an extra spring in series with the compressible cushion of air. The problem in all such 'lumped' approximations – Figure 17 is another case –is knowing how to specify values of equivalent mass and spring constant. The model is illustrated in Figure 36. The diagram models Box C which has only one flexible plate, though this is not a restriction of the model. The oscillating air plug (pale blue) has mass m. The cavity's volume is V and the ambient pressure P. The key assumption is that the plate flexes instantaneously to any change in air pressure – there is no phase lag. This is equivalent to having the lowest normal mode of the plate at a frequency much higher than A0. Thus, if Figure 20 applies to the lowest wood resonance, the air Helmholtz resonance is near 0 on the relative frequency axis where the motion is dominated by the wood's spring and the inertia of the plate has negligible effect. The assumption gains some support from experimental results on Box C such as Figure 8 where the 0-0 breathing mode is at 354 Hz and A0 at 180 Hz.
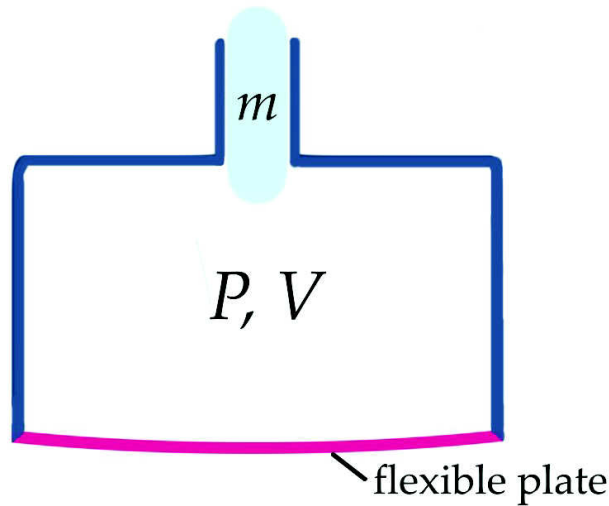

Figure 36: Model of Helmholtz resonator with flexible bottom plate (red).

Suppose that the pressure inside the cavity increases from P to $P+\delta P$. Three things happen:

1. the air in the cavity become compressed,

2. the air plug is pushed out a distance ξ and accelerated,

3. the plate flexes outwards into a dished shaped, so increasing the volume of the cavity by δU.

The total change in volume is $\delta V = A\xi + \delta U$ where A is the sectional area of the neck. Building on the analysis in §5.1, δP and δV are related through the bulk modulus K:

$$\delta P = -K\frac{\delta V}{V} \qquad\qquad Copy\ of\ Eq\ (2)$$

The force on the air plug is $A.\delta P$ and this causes acceleration

$$m\ddot{\xi} = A.\delta P = -\frac{AK}{V}(A\xi + \delta U). \tag{24}$$

We now have to characterise the elasticity of the flexible plate. Since our interest is in volume and pressure changes, let $\mu = \delta P/\delta V$ be the pressure increase needed to produce unit increase in the air volume contained by the dished plate. Then

$$\delta U = \frac{\delta P}{\mu} = -\frac{K}{\mu V}(A\xi + \delta U).$$

Solving for δU

$$\delta U = -\frac{KA\xi}{\mu V}\left(\frac{\mu V}{\mu V + K}\right).$$

Substituting in Eq 24 gives an equation of simple harmonic motion corresponding to Eq 4a

$$\ddot{\xi} + \frac{A^2 K\xi}{mV}\left(\frac{\mu V}{\mu V + K}\right) = 0$$

with natural frequency

$$\omega = c\sqrt{\frac{A\sigma}{L_{eff}V}}, \qquad \sigma = \frac{\mu V}{\mu V + K}. \tag{25}$$

Here the relations $m = \rho A L_{eff}$ and $c^2 = K/\rho$ have been used. Comparing Eq 25 with Eq 4 shows that the plate's flexibility reduces A0 by a factor $\sqrt{\sigma}$.

K and μV both have the dimensions of pressure and each describes an elastic stiffness. The total spring constant k_{12} of two springs k_1, k_2 connected in series is given by

$$\frac{1}{k_{12}} = \frac{1}{k_1} + \frac{1}{k_2}.$$

By analogy

$$\frac{1}{\frac{1}{\mu V} + \frac{1}{K}} = \frac{\mu V}{\mu V + K} = \sigma.$$

As $\mu \to \infty$, $\sigma \to 1$, recovering Eq 4 for a rigid box.

K is known from published data to be $1 \cdot 42 \times 10^5$ Pa at ambient temperature, but we are still left with determining μ. I have used static load modelling in LISA to obtain μ for the two boundary conditions

- fully fixed edges in which displacement in the z (out-of-plane) direction is 0 and also rotation about the local edge as axis is 0,

- semi-flexible edges in which displacement in the z direction is 0, but rotation about the edge is not constrained. This is close to being simply supported.

The former approximates the single back plate of Box C, whilst the second approximates the six plywood sides of Box A (Figure 28). In outline the LISA calculation was as follows. The orthotropic

plate was in the $x - y$ plane. The elastic constants for this pink 3-plywood had been determined in the previous article[14], namely

$$E_1 = 9 \cdot 44, \quad E_2 = 4 \cdot 06, \quad G_{12} = 1 \cdot 04, \quad G_{23} = 0 \cdot 51, \quad G_{31} = 0 \cdot 25 \text{ GPa}, \quad \nu_{12} = 0.$$

I applied the same force in the z direction at every node except on the edge and solved for the z displacements. The sum of these multiplied by the area of plate corresponding to a single node equals the volume within the dish shape which the plate assumes. Therefore μ is {applied load / (plate area × volume in dish)}. For the fully fixed edges $\mu = 2 \cdot 5 \times 10^8$ SI units, whilst for the simply supported edges it decreases to $4 \cdot 25 \times 10^7$.

These values of μ can now be used in Eq 25 to find the percentage reduction in A0 caused by wall compliance. For Box C there is one plate with area $0 \cdot 0544$ m^2 so $\mu V \approx 6 \cdot 1 \times 10^5$ Pa and $\sigma = 0 \cdot 81$. Therefore A0 is 90% of the rigid wall frequency. The only directly comparable experimental measurements are for Cases 19 and 20 in Table 5, from which 156 Hz / 180 Hz = 87%, in remarkable agreement. For Box A it would in principle have been possible to model a uniform outwards force at every node in the finite element model, though extracting the volume change from this would require some careful effort. However, let us just say that only the two 34 by 16 cm plates are significant, and these are adequately approximated by the simply supported condition. It may be that the plate with the aperture does not flex quite as much as the other, but let's say that with two plates the volume change δU is almost doubled. Then μ is halved and $\sigma \approx 0 \cdot 27$, making A0 drop to up to 52%. Again there is only one pair of directly comparable measurements in Table 5, for Cases 17 and 18: 116/166 = 70%. The theory here seems to over estimate the frequency decrease, but qualitatively explains what is seen in practice.

8.2 Coupled oscillations of two masses and springs

I did briefly consider including the inertia of the flexible plate through the two mass-and-spring model in Figure 37. The air plug is shown as a cube of air, mass m, moving through a hole in the top plate and connected to the back plate by a soft air spring of stiffness s. The effective mass of the wooden plate is M and its spring constant is S. The general solution to this is given in textbooks on vibrations. The main difficulty is assigning values to the quantities m, s, M and S.

Take the air plug first. I will base the estimates on Box C at its widest aperture, $d = 61$ mm, $w = 28$ mm. For rigid walls we know from Eqs 3 and 4 that

$$\omega^2 = \frac{KA}{\rho L V} = \frac{s}{m} \quad \text{and} \quad m = \rho L A$$

where L means the effective length of the air plug, Eq 15, and K is the bulk modulus, $1 \cdot 422 \times 10^5$ Pa at 17°C. The sectional area A is 1448 mm^2 and from Eq 15 $L \approx 2 \cdot 9 + 2/3\sqrt{(61 \times 28)} \approx 30$mm. $\rho = 1 \cdot 22$ kg/m^3 so m is about 54 mg. The formulae above give

$$s = \frac{KA^2}{V} \approx 122 \text{ Pa/m}.$$

These values of m and s would predict the Helmholtz frequency to be 240 Hz. LISA predicts that A0 should be at 220 Hz (Case 22 in Table 5), and this implies that s is 103 Pa/m.

---

[14]'The Vibration of Plywood Plates by Experiment and Finite Element Analysis: Edge Constraints and Box Structures'.
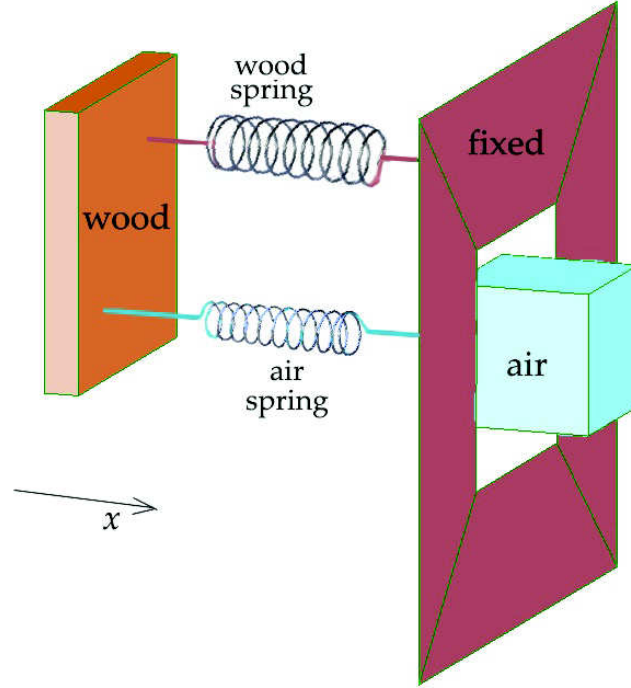
Figure 37: A system with 2 degrees of freedom modelling interaction between air and the box walls.

M and S are more problematical because the plate is precisely that – a plate covering an area and held at the edges, not a rigid body whose displacement can be specified by a single value. Moreover, M and S are intended to represent the plate at the frequencies of A0 and the wood 0-0 and possibly higher modes. However, it cannot be assumed that one value of M and one of S can apply over a wide frequency range. Here are three ways of looking at them:

Case 1 : In §8.1 $M = 0$ and S is represented by μV, an equivalent bulk modulus whose value is calculated at zero frequency.

Case 2 : The actual mass of the flexible plate of Box C is 94 g and the 0-0 mode is at 354 Hz, so $\omega^2 = S/M$ would imply that $S = 4 \cdot 65 \times 10^5$ N/m.

Case 3 : Figure 8, §2.2 shows the effect on the 0-0 frequency of adding masses in 6 g steps. This can be modelled in LISA. Suppose that M_a is added with Plasticine or otherwise. The formula $\omega^2 = S/(M + M_a)$ can be rewritten as a straight line

$$M_a = \frac{S}{\omega^2} - M.$$

Therefore plotting the added mass against $1/(2\pi f)^2$ should give a straight line graph with gradient S and intercept M.

Figure 38 shows such graphs for the experimental values in Figure 8 and for finite element predictions using the elastic constants in §8.1 above, and applying the extra mass in a small patch near the centre of the back plate. The LISA model calculates the plate's normal modes assuming it to be in vacuum, while the experiments of course had air inside and around the box. The finite element prediction is that M is $12 \cdot 5$ grams and the spring constant $S = 5 \cdot 5 \times 10^4$ Pa/m, whilst the experimental values
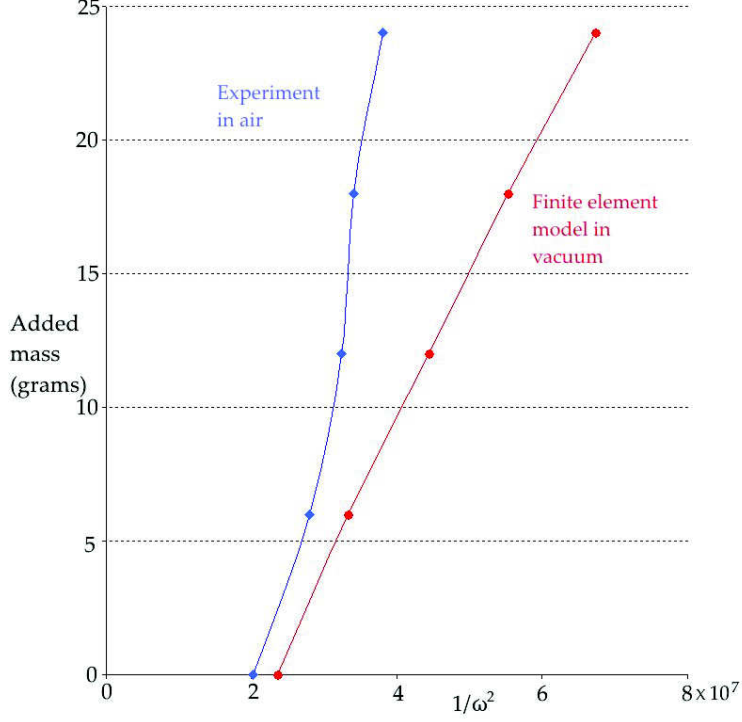
Figure 38: Effect on breathing-mode frequency of adding mass to the back plate of Box C .

give $M \approx 30$ g, $S \approx 14 \cdot 4 \times 10^4$ Pa/m. It is remarkable how smaller M is than the actual 90 g mass of the plate.

However, things are not straightforwards. I carried out more LISA calculations to examine the effect of spreading the added mass over a larger area. Not surprisingly, adding all the mass towards the centre, where the displacement, velocity and acceleration are greatest, has a much larger effect than adding it around the edge. With all mass added only to the central node the graph extrapolates to $M = 12$ g with gradient $S = 5.0 \times 10^4$ N/m. At the other extreme, spreading the added mass uniformly over the plate gives $M = 91$ g, the actual weight of the plate, and $S = 3 \cdot 89 \times 10^5$ N/m. These correspond to LISA's predicted frequency for 0-0 of 328 Hz.

To see how these options affect the model's predictions it is necessary to solve the equations of motion for Figure 37. Suppose that a periodic force $F \cos \omega t$ is applied to the wooden plate. Use X and x for displacements of plate and air plug respectively. Include a damping force of $R\dot{X}$ on the wood's spring, and one of $r\dot{x}$ on the air's spring. Then the equations of motion are

$$F \cos \omega t - SX + s(x - X) - R\dot{X} + r(\dot{x} - \dot{X}) = M\ddot{X}, \qquad (26a)$$

$$-s(x - X) - r(\dot{x} - \dot{X}) = m\ddot{x}. \qquad (26b)$$

In the usual way look for periodic solutions in which all parts move at the same frequency. Substituting $X = A \exp i\omega t$, $x = a \exp i\omega t$ leads to two simultaneous linear equations which in matrix form are

$$\begin{pmatrix} S + s - M\omega^2 + i\omega(R + r) & -s - i\omega r \\ -s - i\omega r & s - m\omega^2 + i\omega r \end{pmatrix} \begin{pmatrix} A \\ a \end{pmatrix} = \begin{pmatrix} F \\ 0 \end{pmatrix}$$

Our interest is in the steady state behaviour so ignore the transient solution for $F = 0$. Also, the damping terms make the solution look very complicated. We know from §5.2 that R and r broaden

and decrease their respective resonances without shifting the peak frequency much, so for the time being set $R = r = 0$. The amplitudes A and a are complex quantities representing both amplitude and phase relative to $F \cos \omega t$. Their magnitudes are

$$A = \frac{F(m\omega^2 - s))}{H}, \quad a = \frac{Fs}{H}, \quad H = Mm\omega^4 - (Ms + ms + mS)\omega^2 + Ss. \tag{27}$$

The denominator is a quadratic in ω^2 and clearly the resonant frequencies occur where it is zero. Write the above in terms of the resonant frequencies of the uncoupled wood and air mass-spring systems, $\omega_w^2 = S/M$, $\omega_a^2 = s/m$

$$\frac{A}{F} = \frac{\omega^2 - \omega_a^2}{H'}, \qquad \frac{a}{F} = \frac{\omega_a^2}{H'}$$

$$H' = M\left[(\omega^2 - \omega_w^2)(\omega^2 - \omega_a^2) - \frac{s}{M}\omega^2\right]. \tag{28}$$

In this form it is easy to see that if s/M is negligible,

$$\frac{A}{F} \to \frac{1}{M(\omega^2 - \omega_w^2)}, \qquad \frac{a}{F} \to \frac{\omega_a^2}{M(\omega^2 - \omega_w^2)(\omega^2 - \omega_a^2)} \tag{29}$$

which tend to infinity at the natural frequencies of the separated wood and air systems. s/M therefore determines the interaction between the air and wood resonances.

For a numerical illustration let us take at face value the frequencies of A0 at 220 Hz and wood 0-0 at 328 Hz predicted by LISA for Box C with the 61 by 28 mm aperture (recall §2 and Table 5, Case 22). Normalise with respect to the Helmholtz frequency for rigid walls, ω_a, by letting $\omega_a = 1$. The ratio ω_w/ω_a is $1\cdot49$. Figure 39 shows how the two resonances diverge as the coupling s/M increases. The experimental values of A0 and 0-0 are 180 Hz and 354 Hz. Unfortunately these do not correspond to a single value of $y = s/M$. For A0 to fall to $0\cdot82$, s/M must be $0\cdot77 \equiv 168$ Hz, but for 0-0 to rise to $1\cdot61$ requires s/M be to only $0\cdot23 \equiv 50$ Hz. At the beginning of this
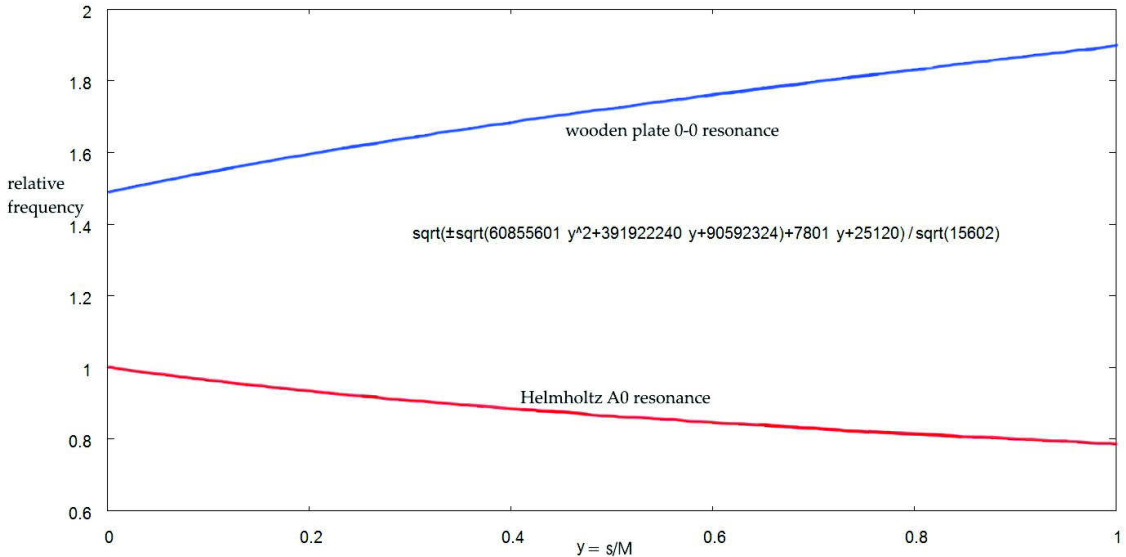

Figure 39: Increase in plate 0-0 modal frequency and decrease in A0 as wood-air coupling s/M increases, normalised to A0=1.

46

sub-section §8.2 s was estimated by LISA to be 103 Pa/m. 50 Hz would then require M to be only 1 gram, which seems nonsense – it cannot even be reconciled with the 12 g limiting value when all mass added to the plate is placed in the very centre.

I cannot explain why this two mass-and-spring model is so poor. It seems to be saying that the plate's mass M is essentially zero, and hence that a two-mass-two-spring model is not appropriate. Probably the most we can claim is that it shows that the air and wood resonances push each other apart in frequency. The one-mass-two-springs model of §8.1 is a more reasonable quantitative model.

8.3   Other theories of the elastic Helmholtz resonator

Several researchers have been inspired by the pioneering work of Saunders and Hutchins (§4) to explore the A0 and A1 air resonances and the main wood resonance of violins by experiment and theory. Much use has been made of equivalent electrical networks to model the acoustics, starting probably with John Schelleng (J Acoustic Soc America (JASA) Vol 35 No 3 1963 326-338). Nearly 30 years later E. Shaw (JASA Vol 87 1990 398-410) developed an alternative '2 degrees of freedom' model which he applied to model Hutchins' 'Swiss-cheese' violin with 65 holes in its ribs. This treated the violin as made of its two bouts, treated as upper and lower spring-like capacitances, connected by a channel under the bridge which acts as a mass. In this way it can deal with non-uniform pressure distribution within the cavity, which LISA also predicts (see Figure 34 for A0, 35 for A1). It predicts that in the A0 modes the pressure in the upper volume is 30% higher than in the lower. This is consistent with the LISA solution in Figure 34. This ventilated violin was studied again by Weinreich, Holmes and Mellody (JASA Vol 108 2000 2389-2402). They interpret the modes of vibration of a violin in terms of a revised set of 'dynamic' basis modes which are characteristic of the instrument and recognise that, for instance, A0 is influenced by wall flexibility. Their experimental measurements, however, are only on the Swiss cheese violin.

George Bissinger (JASA Vol 100 No 3 1996 1835-1840) carried out numerical calculations of standing waves in a closed, rigid, violin-shaped cavity. The method involved internal scattering of standing wave resonances introduced by point source excitation of the cavity, using the BEMAP boundary element program rather than finite elements. He used it to examine the effects of plate arching and rib height on A0 and A1. Later he made a violin-shaped box out of aluminium (JASA Vol 104 No 6 1998 3608-3615) to study coupling between A0 and A1 and relate experimental measurements with an extension of Shaw's equivalent electrical network. Later still Bissinger made acoustic pressure measurements on a series of violin family instruments to quantify further the effect of wall compliance on the cavity air modes (JASA Vol 113 No 3 2003 1718-1723). He finds that A0's dependence on cavity volume is essentially as $V^{-1/3}$ and not the $V^{-1/2}$ predicted by simple theory for rigid walls as in §5.1. Indeed, he says that coupling of A1 and A0 would make the dependence as $V^{-1/4}$ for rigid walls.

There is a wealth of detail in these papers, with many effects and subsidiary effects being described, variously modelled and related to one another. Broadly their collective thrust is that A0 is important for loudness and tone in the lower register, that it is linked through the geometry of the cavity to A1, and is reduced by compliance of the cavity walls.

Coming from a very different starting point, the theory of a resonator with flexible elastic walls has been analysed using sophisticated mathematics by Andy Norris and Gerry Wickham[15] [16]. This is a mathematically exact treatment, unlike the rather heuristic treatments noted above. They first formulate the problem for a hollow thin-walled shell of arbitrary geometry, then particularise to a spherical elastic shell with a circular hole cut into it, immersed in a fluid and with a plane compression wave incident. Damping is only by radiation. The similar situation with a rigid hollow sphere is solved as a 'problem' example by Morse and Ingard on pages 692-694 of their classic tome 'Theoretical Acoustics' (McGraw-Hill, 1968). Norris and Wickham formulate the scattering problem exactly as an integral equation across the aperture using mathematical devices previously developed by Wickham. As expected from the geometry, the exact solution is given as sums of spherical harmonic functions. They find that the effective impedance of the fluid filled cavity is the result of the enclosed fluid and shell acting in series; this is also what I found in my simple model of §8.1. They also prove that A0 must always be much lower than the lowest structural frequency of the resonator, so A0 and 0-0 will always be distinct. Numerical examples of exact solutions are given for steel shells in water, but, as in several of their other papers, the authors are mainly interested in uniformly valid asymptotic expansions for approximating the field at long wavelengths and small apertures.

I will give a summary of Norris and Wickham's asymptotic results because they are exact within their assumptions. I must say, however, that, regrettably, entering numerical values for Box C does not predict a noticeable lowering of A0 and so does not fit my experimental measurements. I cannot explain why this should be.

Using their notation, the spherical shell has radius a and wall thickness $h \ll a$. The cavity's volume V is therefore $4\pi a^3/3$. The aperture is circular and defined by the semi-angle α which it subtends at the centre of the sphere. The spherical area of the opening is then found by integrating the element of surface area $a^2 \sin\phi \, d\phi \, d\theta$ to be $S = 2\pi a^2(1 - \cos\alpha)$. A plane wave of radian frequency ω is incident normal to the plane of the aperture. They find the Helmholtz frequency and Q factor to be

$$\omega_{A0}^2 \;=\; c^2\,\frac{R_0\,S}{V\,\delta}, \qquad\qquad Q = \frac{4\pi}{R_0\,k_0^3\,V}. \tag{30}$$

Compare these with Eq 4 of §5.1 and Eq 20 of §5.4. δ is the effective length of the air plug given by

$$\frac{\delta}{a} \;=\; \left(\frac{\pi}{2} - \alpha\right)\sin\alpha \;+\; \sin^2\frac{\alpha}{2} \;+\; \frac{6}{5}R_0\bar{R}_0\sin^2\frac{\alpha}{2} \;-\; \frac{1}{2}R_1\sin^2\frac{3\alpha}{2}\,. \tag{31}$$

For a rigid shell R_0 and R_1 are both 1. For a flexible shell they are

$$\frac{1}{R_0} \;=\; 1 \;+\; \frac{a}{h}\,\frac{3\rho c^2}{2(1+\nu)\rho_s\,c_s^2} \tag{32}$$

$$\frac{1}{R_1} \;=\; 1 \;+\; \frac{a}{h}\,\frac{\rho}{2\rho_s}\;.$$

$$\bar{R}_0 \;=\; R_0 \;+\; (1 - R_0)\,\frac{4}{5(1+\nu)}\,\frac{c^2}{c_s^2}\;.$$

---

[15]Gerry Wickham was a personal friend of mine. Gerry and I collaborated over about 12 years on a number of projects to do with elastic wave scattering applied to ultrasonic non-destructive testing of metals in industry, and in the course of this my company supported about 10 research students of Gerry's. He was an able and enthusiastic mathematician who was appointed professor at Brunel University after 26 years in the Maths Department, University of Manchester. He died suddenly of a brain haemorrhage on Christmas Eve, 1995, aged only 52.

[16]J Acoust. Soc. Amer. Vol 93, No 2, February 1993

Here subscript $_s$ refers to the shell. ρ is the density, c the velocity of sound and ν Poisson's ratio. c_s is related to Young's modulus E and density through $c_s^2 = E/[\rho_s(1 - \nu^2)]$. So Norris and Wickham express the compliance of the shell in terms of its velocity of sound and density.

Air has these values in SI units : $\rho = 1 \cdot 26$, $c = 341 \cdot 5$.

For the plywood $\nu \approx 0$ and $E = 9 \cdot 4 \times 10^9$ so with $\rho_s = 596$, $c_s = 3970$.

$h = 0.00291$ m so we are left only with finding equivalent values for a and α, seeing that Box C is a cuboid, not a sphere, and has an oval opening, not a circle. I'll choose a to give the same volume as Box C, which is $V = 0 \cdot 002448$ m^3; then $a = 0 \cdot 0836$ m. The actual area of the aperture is 1448 mm^2, equivalent to a circle of radius $0 \cdot 0215$ m. This radius, taken with the above equivalent radius of the sphere, would mean $\alpha = 0 \cdot 26$ radians $\approx 15°$. This says the aperture subtends about 30° at the centre of the sphere, which strikes me as rather large. Nevertheless, let's work with these equivalent values.

Substituting in Eq 32 gives $R_0 = \bar{R}_0 = 0 \cdot 9993$ and $R_1 = 0 \cdot 97005$, virtually the rigid wall values. Then δ, from Eq 31, is also no different from its rigid wall values and the formulae, despite their rigour, predict no change for Box C. C'est la vie!

9   Conclusion

This article has examined the resonances of the air cavity of a violin and studied the lowest frequency oscillation, A0, in some depth. This explains part of the role of the f-holes, though not their effect on vibration of the top plate. The following main points seem clear:

1. The A0 air resonance at about 270 Hz (C sharp) in a violin is indeed a Helmholtz resonance in which the air in the cavity behaves as a spring causing a plug of air near each f-hole to oscillate.

2. The frequency is governed by the geometry of the instrument and the size of the holes. To first order several holes act as one having the aggregate area and produce only one resonance. Formulae Eq 4 and Eq 18 give quite accurate predictions for resonators with rigid walls.

3. A0 of a violin can be adjusted by widening or partially covering the f-holes. Widening sharpens the note and covering flattens it. If one f-hole is completely covered, A0 drops by about a musical fourth.

4. The sound amplitude of A0 is roughly proportional to the total area of the holes, so covering them diminishes their contribution to tone.

5. I have suggested that a stronger A0 resonance yet with a large Q, so covering a wider frequency range, might be achieved by significantly increasing the opening of an f-hole and lining it was a cloth sleeve to form a non-rigid neck. Perhaps I will sacrifice a violin to this theory.

6. A0 can be measured in two ways using simple equipment: a) by an internal electret microphone with external excitation through the air from a nearby loudspeaker, and b) by an external microphone when the violin bridge is driven by an electromagnetic vibrator.

7. Some plate modes can be distinguished from air cavity modes by adding small masses to the plates and observing the decrease in resonant frequency.

8. A0 is quite a narrow resonance – about a semitone either side of C$\sharp$. Q is governed mainly by viscous losses at the holes rather than by sound radiation. There are minor peaks on the lower

shoulder of this resonance. I have no explanation for either the origin or musical importance of these.

9. Though the Helmholtz resonance is widely regarded as crucial to supporting the loudness and tone in the lower register of violin family instruments, my own subjective listening tests on a violin played normally with the *f*-holes variously obstructed led to no clear impressions. With one hole covered the tone on the lowest string seemed rather nasal, and thin with both covered.

10. Finite element modelling with the LISA program gives solutions of Helmholtz's equation which are in good agreement with experiment on nominally rigid structures, though A0 is about 4% high.

11. Crucially, the A0 frequency is strongly influenced by the flexibility of the wooden box. Mathematical treatments which assume rigid walls give an upper bound. In the rectangular box made from with 3 mm thick 3-ply, A0 was only about 70% of the rigid wall value. The simple one-mass-two-springs model, supported by finite element values of plate deformation, described in §8.1 has given quite good agreement with experiment.

Despite these studies I remain unsure of the importance of the *f*-holes and the air resonances in determining the tone of a violin or viola during normal play. How can such a narrow (±one semitone) resonance about an infrequently played note, C♯, benefit the tone over the whole lower register of the instrument? Though stimulated as a transient by each note played, it does not persist long enough to make a perceivable difference. I intend a future paper to look further into violin tone.

John Coffey, Cheshire, England, April 2013.